Preliminary study of the effects of vortex generators in ultralight aircraft

Degree:
Grau en Enginyeria en Tecnologies Aeroespacials (GRETA)

Author:
Oriol López Calle

Director:
Rafael Weyler Perez

Co-director:
Montserrat Sanchez Romero

Call for work delivery:
June 2015

Content of this volume:
DOCUMENT 1: REPORT

"You know that you have landed with the landing gear up when it takes full power to taxi to the hangar"

Acknowledgements

There is a bunch of people who contributed to this study. I am very grateful to my director Rafael Weyler for his guidance, sincere opinions and smart contributions to the paper. I also want to mention his great camera and co-piloting skills – thank you!
I also want to thank David del Campo for his great aerodynamic knowledge contribution and his useful CFD related advices.
Antonio Marcos has been a key piece to make the experimental tests happen, his knowledge, passion and restlessness in aviation are priceless. I am glad to have been taught to fly by such an experimented and skilled pilot.
Montserrat Sánchez, Daniel García, Arnau Serra, Luis Manuel Pérez, Laura and my family have definitely made this possible.
In return, my compromise is to share my research and my passion for aviation the same way everyone shared their time and opinions with me.

Contents

Figure index

Table index

PART I: INTRODUCTION

1.1 Aim

The aim of the study is to set the criteria and procedures needed to properly study vortex generator's behavior and performance for a given ultralight aircraft model.

1.2 Scope

The scope of the study is to test different simulation parameters and establish reliable criteria in order to obtain reasonable results in three-dimensional Computational Fluid Dynamics analysis.

The final aim of the project should be simulating different configurations of vortex generators in a given ultralight aircraft model in order to compare them and extract conclusions regarding these devices in ultralight aviation. This goal is unachievable from an academic perspective due to computing power limitations, but the paper will focus on the pre-processing of CFD simulations and result analysis.

If those steps are done correctly, the future tasks part should be all about parallel computing expensive simulations.

According to this, the steps below will be followed in this paper:

- Theoretical approach to vortex generator operating principle.
- State of the art on the use of the vortex generators.
- Analysis of the criteria to carry out meaningful analysis in 2D.
- 2D airflow simulations across the given lifting surface and result verification.
- Analysis of the criteria to carry out meaningful analysis in 3D.
- Experimental flight tests with and without vortex generators in a given ultralight model and the pertinent experimental data contrast.

1.3 Requirements

This paper consists in a qualitative approach to CFD airfoil and wing simulations, thus requirements cannot be expressed numerically because no numerical results will be obtained in a preliminary study.

- Achieve reasonable and accurate criteria to carry out CFD simulations of a 2D airfoil stall situation.
- Identify flow separation and airfoil stall in 2D simulations.
- Achieve reasonable and accurate criteria to carry out CFD simulations of a 3D wing stall situation with and without vortex generators.

- Experimentally validate some or all of the data found in the bibliography regarding vortex generators effects. Detect a noticeable (over 4 km/h) loss in stall speed with VG implementation.

1.4 Justification

The justification of the project arises with the necessity of finding a good compromise solution on the configuration of vortex generators. As this device uses a rather old aerodynamic technology, the pros and the cons of the implementation of the device have to be shaped carefully. This is something that is rarely done in experimental ultralight aviation, and the final target of the study should be finding enough evidence of an optimized and useful vortex generator configuration. Commercial aviation uses of this device are common and this study can also be oriented as a previous step towards there. The use of those devices causes a delay in the detachment of the boundary layer thus a lower stall speed, which basically endows the aircraft lower takeoff and landing distances and more aerodynamic control at low speeds. The drawback of the system is generally an increase in drag, which means lower cruising speeds. Price, durability and other factors regarding the devices have to be taken into account too. Deeper research and optimization can be carried out in this field, as it also has applications in military and commercial aviation.

Vortex generators have different shapes, sizes, positions, and are made of different materials, so there is a need of shedding some light on the proper use of those devices in ultralight aircraft. Although the initial analysis would be made for a given standard ultralight model (thus for a specific airfoil and wing) in order to narrow the project's scope, results could be extrapolated to other similar aircraft.

Preprocessing simulations - which includes settling the basic concepts, meshing methods and choosing turbulence models, among other tasks - and post-processing them is as important as the actual simulation. In finite elements analysis it usually happens that results differ from reality and authors are focused on the simulation stage to find out what is going on. Sometimes the cause of massive differences between simulations and reality is the mesh, or a wrong physical concept behind the simulation. This is called the “garbage in, garbage out” effect, which states that sometimes, even using very powerful computers, simulation results will not be good as long as the grid or the equations used by the solver are not optimal.

The experimental part of the project is the last but not the least. Its aim is to capture the approximate stall speed reduction by adding vortex generators to the ultralight that will be studied in the simulations. An order of magnitude of the results that should be found through simulation can be obtained. This information can also be used to determine how far from reality are simulation results with inappropriate and coarse setups.

This paper's aim is to evidence the importance of this previous step and provide the reader with an accurate work to understand the principles on how to tackle this particular challenge.

PART II: PREVIOUS STUDY

2.1 Vortex Generators basics

2.1.1 Previous study justification

This paper's aim is not to jump on the simulation stage straight away as there are a lot of obstacles that need to be dodged first. The previous study of the vortex generators devices and the effects that they produce in the aircraft wing is a must. The previous study also focuses on the physical environment of a 3D study to provide the future simulations with enough knowledge to tackle the problem properly and obtain reasonable and accurate results.

2.1.2 Definition

A vortex generator (VG) is a small, fin-like device attached to a lifting surface in order to control its aerodynamic boundary layer. Its main goal is to delay flow separation and aerodynamic stalling. By doing so, different results such as better aerodynamic performance, better climb capacity, and lower stall speeds can be expected, along with all its positive and negative secondary effects. When mounted on the tail of the aircraft, VGs increase rudder effectiveness and lower minimum control speed (Vmc).

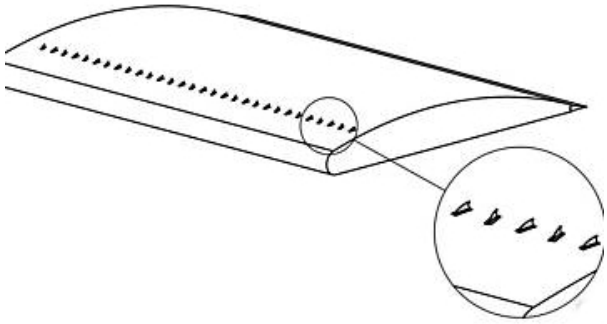

Figure 1 Finite wing with Vortex Generators

Figure 2 Close-up image of triangle-shaped vortex generators

Actually, vortex generators can be used in wind turbines, car fuselages and rotor blades, and even in their applications in aircraft design their position can vary widely: from the leading edge of the wing to the inboard side of the nacelle.

As the final aim of the study is to implement those devices in ultralight aircraft, the paper will focus on how to tackle a study of the effects of a **Passive Vane Vortex Generator.**

2.1.3 The basics

A Passive Vane Vortex Generator consists of a small vane placed in a determined position of the extrados of a wing - usually pretty close to the leading edge of the airfoil. They are frequently used among a high number of the same devices, usually placed in groups of two. VGs are installed normal to the surface, with a vane angle of incidence α towards the mean-flow direction. Flow-separation control with passive VGs is by far the cheapest and fastest way to equip fuselages in the aeronautic field therefore it's commonly used in the industry.

VGs generate a stream wise vortex without requiring addition external energy - that is why they are called passive vortex generators. The benefits of using VGs come along with a somewhat increased overall drag. To avoid this penalty there is the option to retract the VGs when they are not needed, but this will not be taken into account, as it is not seen as a viable solution in ultralight aviation.

2.2 Computational Fluid Dynamics

This is a necessary introduction to deal with fluid dynamics and aerodynamics along the project. More information or data may be consulted in reference [1] to properly follow the study.

2.2.1 Introduction to CFD

As this whole study is based in Computational fluid dynamics (CFD), it is necessary to settle the basics and mention the governing equations used to approach the problem. [2]

CFD is the process of suing numerical methods to solve fluid flow problems.

The Navier Stokes equations, which describe the physics of fluid flows, cannot be solved analytically for the case that will be studied. An approximate solution is then required and the most relevant equations are the conservation of mass:

$$\frac{\partial \rho}{\partial t} + \nabla \cdot (\rho v) = 0$$

And the conservation of momentum

$$\rho \frac{\partial v}{\partial t} + \rho(v \cdot \nabla)\mathrm{v} = -\nabla \mathrm{p} + \rho \mathrm{g} + \nabla \cdot \tau$$

where

$$\rho = density\ of\ the\ fluid\ in\ kg/m^3$$
$$v = velocity\ vector\ in\ m/s$$
$$p = fluid's\ pressure\ in\ Pa$$
$$g = gravity\ in\ m/s^2$$
$$\tau = stress\ tensor\ in\ Pa$$

These equations are both coupled and non-linear. Solutions for such complex flows are obtained by discretizing the equations, and solving them through an iterative process. For the computer to be able to work with the equations, the entire domain, including the geometry, needs to be discretized. The discrete model of the computational domain is called a grid or a mesh.

There are three steps in solving a CFD problem:

1. Create a grid for the geometry
2. Solve the desired equations using a solver and a model
3. Post-process the results
4. Verify and validate the code by comparing the models results to experimental results.

Different models are available on the simulation software to tackle the problem and capture the desired physic effects, and they will be discussed in the second part of the paper.

2.2.2 CFD approach

This paper has an academic background and it obviously has some limitations. The most important limitation that this kind of projects face is the lack of computer processing power to carry out the simulations.

This paper is intended to give a reasonable and accurate approach on how to study 3D vortex generators effects. As it will be clearly explained later on, CFD simulations require a lot of processing power to accurately describe what is happening in every single node of the geometry; what is the value of the pressure, the velocity, and any parameter and variables. The situation gets even more complicated when three-dimensional problems like VGs effects want to be approached. High quality grids and a very high number of elements are needed to obtain reasonable results.

The amount of precision needed to simulate VGs effects is so beyond academic possibilities that this paper wants to develop a path to be followed to carry out good quality and reasonable simulations, not random discretizations and plotted results with no verification.

Some results can still be obtained and especially 2D simulations are affordable for a normal processor. However, every result must be analyzed and validated, and particularly 3D results of the simulations carried out must always be written with a question mark. This is the reason why this work will focus on the simulation criteria more than in the results themselves; computational power and the time-frame is what it is and this cannot be changed.

2.2.3 The boundary layer

The most important part of the simulation process is choosing good criteria to define the discretization that will result in the grid of the geometry. As this study is trying to capture turbulent and boundary layer related effects, it is important to emphasize in the study of phenomena occurring there, in order to create a proper mesh.

The boundary layer is defined as the layer of air from the surface of the wing to the point where there is no measurable slowing of the air due to viscosity of the air and friction of the wing. Thus it is the region in a flow close to the wall where viscosity must be taken into account. A more practical definition of an airfoil boundary layer is where the parallel velocity is less than 99% of the free stream velocity:

$$u(y) < 0.99U_0$$

At the wall, there is a no-slip boundary condition that dictates that

$$u(y)|w = 0$$

while away from the wall it eventually reaches U_0.

The reason that explains why the fluid has a certain velocity profile in the boundary layer is the shear stress caused by the boundary conditions. This can be divided in two terms:

- Viscous stress ($\mu\frac{d\bar{u}}{dy}$) is the part of the stress that can be attributed to the strain rate, the rate of change of deformation over time. In other words, it is the component that corresponds to the viscous friction between the fluid and the wall.
- Reynolds stress ($-\rho u'v'$) is the component of the total stress in a fluid obtained from the averaging operation over the Navier-Stokes equations to account for turbulent fluctuations in fluid momentum. It is strictly related to turbulent disorders.

The relationship between them determines the transition process from zero velocity at the wall to free-stream velocity, and thus also the height and shape of the boundary layer. Figure 3 gives an example of the relationship between the two stresses.

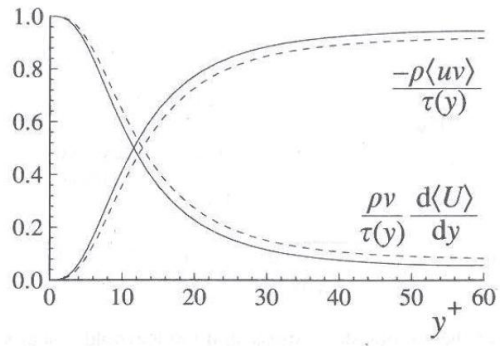

Figure 3: Profiles of the fractional contribution of the viscous and Reynolds stresses to the total stress. DNS data of Kim et al. (1987): dashed lines, Re=5600; solid lines, Re=13750. From [3].

In highly viscous flows the viscous stresses will dominate over a larger range, and boundary layers will be larger than in low viscous flows.

2.2.4 Transition from laminar to turbulent flow

The laminar boundary layer flow is a very smooth flow, with no disruption between the layers. It has low skin friction drag but it is unstable, which means that flow separation is easier when it has laminar behavior at high angles of attack. Laminar flow airfoils tend to provide low drag at cruise but nasty stall characteristics.

Turbulent boundary layer is characterized by chaotic property changes. The flow has more energy and has rapid variations of pressure and flow velocity in space and time - turbulence is complex and therefore turbulent flow is more complex to simulate. In turbulent flow, drag caused by boundary layer skin friction increases.

Figure 4 shows a good intuitive approach of the transition process.

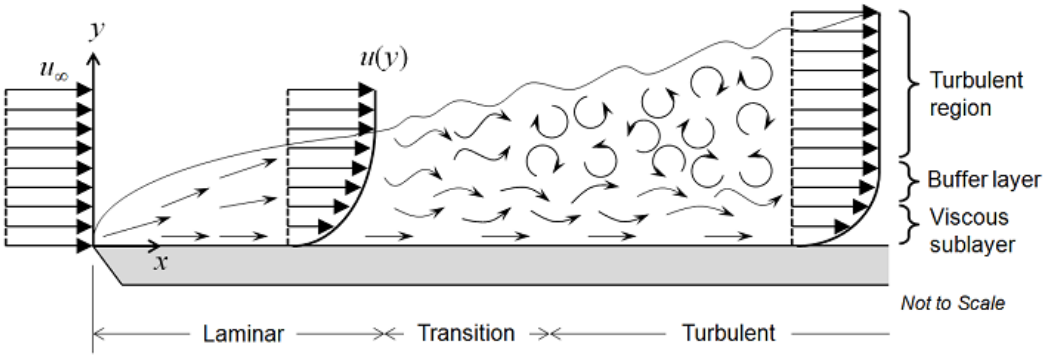

Figure 4: Schematic process of laminar to turbulent flow transition. Not to scale.

Back to the physic and more accurate approach, there is not a universal way to determine the transition point, but the Reynolds number is an important parameter.

$$Re = \frac{\rho U L}{\mu}$$

where

$$U = characteristic\ velocity\ of\ the\ system\ in\ m/s$$
$$L = characteristic\ length\ of\ the\ system\ in\ m$$
$$\rho = density\ of\ the\ fluid\ in\ kg/m^3$$
$$\mu = dynamic\ viscosity\ of\ the\ fluid\ in\ \ kg/(m \cdot s)$$

Laminar flow occurs for low Reynolds numbers, while turbulent flow occurs for high Reynolds numbers.

An illustration of the increase and amplification of small disturbances along the flow thus transition from laminar to turbulent flow is shown below.

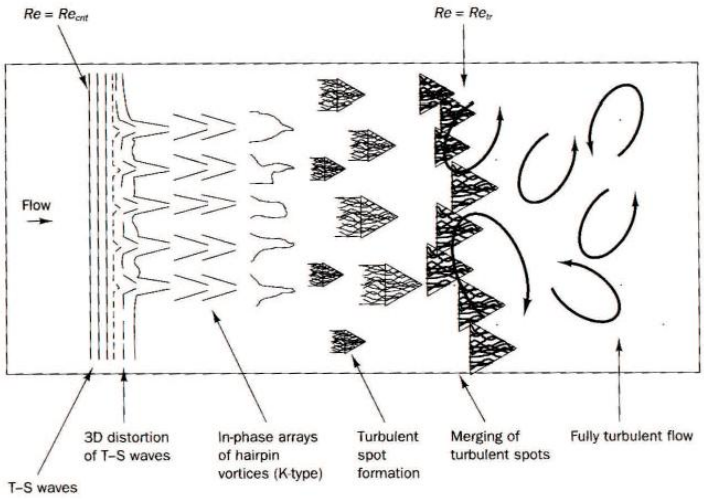

Figure 5: Sketch of the transition from laminar to turbulent flow on a flat plate.

2.2.5 Coefficients

2.2.5.1 Definition

[2] The net force acting on an airfoil is normally decomposed into two parts, the lift force, which is perpendicular to the free stream velocity, and the drag force, which is parallel to the free stream flow.

Drag is the sum of pressure forces and viscous forces acting on the airfoil in the direction of the free stream flow. The viscous forces are always acting in the same direction as the free stream velocity, hence increasing drag. Thrust given by the propeller is defined as negative drag.

Lift is generated due to a pressure difference between the upper and lower side of an airfoil. The pressure is lower on the suction (normally upper) side, than on the pressure (lower) side.

Both lift and drag can be non-dimensionalized into lift and thrust coefficients as:

$$C_l = \frac{l}{\frac{1}{2}\rho U_0^2 c} \quad and \quad C_d = \frac{d}{\frac{1}{2}\rho U_0^2 c}$$

$$L = lift\ force\ per\ unit\ length\ in\ the\ spanwise\ direction\ (N)$$
$$D = drag\ force\ per\ unit\ length\ in\ the\ spanwise\ direction\ in\ N$$
$$\rho = fluid\ density\ \ in\ kg/m^3$$
$$U_0 = free\ stream\ velocity\ in\ m/s$$
$$c = chord\ length\ in\ m$$

2.2.5.2 Angle of attack dependence

The lift coefficient increases along with angle of attack until the critical angle of attach is reached, when stall occurs (see section 2.2.6).

The critical angle of attach is the angle of attack which produces maximum lift coefficient. Figure 6 shows the typical angle of attack against lift coefficient relationship.

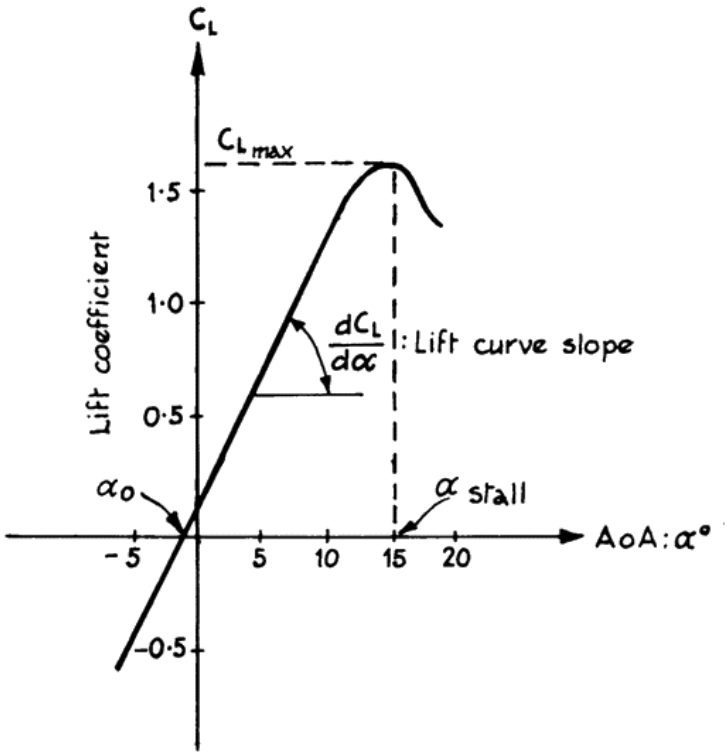

Figure 6: Lift coefficient vs angle of attack for a 2D flow over an airfoil.

2.2.5.3 2D and 3D lift coefficients

Note that so far only section coefficients have been seen. They are based on two-dimensional flow over a wing of infinite span and non-varying cross-section so the lift is independent of spanwise effects and is defined in terms of lift and drag forces per unit length. They are used for two-dimensional analysis.

What really matters when the whole aircraft is being analyzed is the lift coefficient distribution along the wing for every single section, which can be computed as the integral of the airfoil lift coefficients along the different chord lengths. The useful way to deal with wing lift coefficients is computing them as a result of the whole lift in the aircraft. Same applies for the drag coefficient.

$$C_L = \frac{L}{\frac{1}{2}\rho U_0^2 S}$$

$$S = wing\ area\ in\ m^2$$
$$L = lift\ force\ on\ the\ whole\ wing\ in\ N$$

Ideally, airfoil lift coefficients c_l and wing lift coefficients C_L should be equal. However, three-dimensional vortex effects on the wings entail a loss in the wing lift coefficient C_L as two-dimensional lift coefficients don't take into account 3D imperfections.

In normal operating conditions, the wing will have high pressure on its lower surface and a low pressure on its upper surface. This same pressure difference causes flow from the underside of the wing to the upper side of the wing around the wing tips. [4]

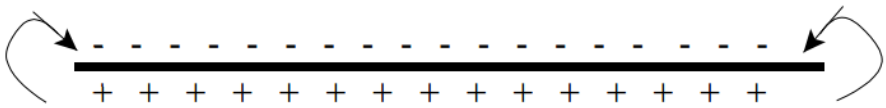

Figure 7: Direction of wing tip vortex due to difference of pressure betewen upper and lower surface.

This type of flow swirls off the tips of the wing in the form of vortices. In fact there is a vortex distribution across the entire span of the wing with the strongest vortices at the wing tips. These vortices trail downstream behind the wing and rotate in the direction shown in the figure. Vortices on the right hand side of the wing (looking from the rear) rotate counter clockwise, and those on the left hand side of the wing rotate clockwise. The general result is that the vortices induce a downward flow at the wing interior. This downward flow is called downwash, and it influences the flow in front of, at, and behind the wing. This downward flow causes a change in the local wing angle-of-attack such that the wing sees a different angle-of-attack than the one that it sees with respect to the free stream.

3D lift coefficient C_L is usually about a 20% lower than the airfoil predicted c_l lift coefficient, and stall occurs about 2-3 angle of attack degrees later due to the effect previously described. Implementing vortex generators has actually a similar effect but on a tiny scale in the extrados of the wing.

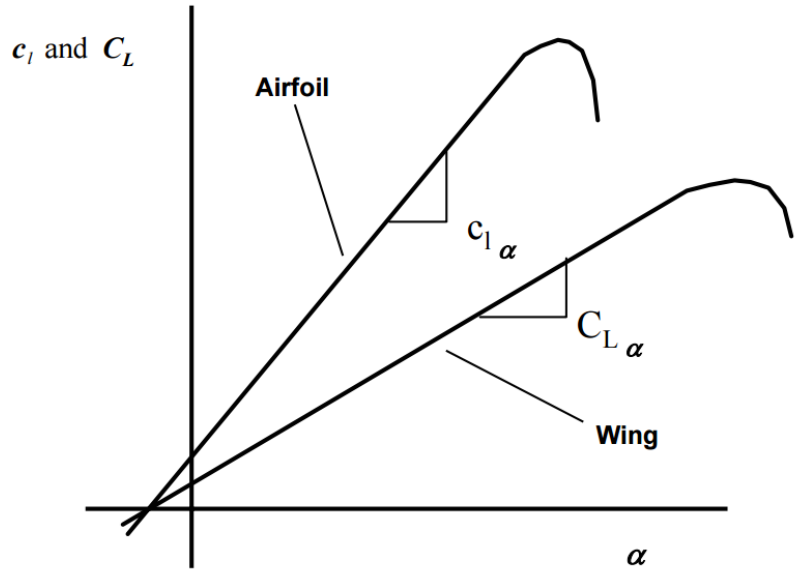

Figure 8: Graphical comparison of airfoil and wing lift coefficients (c_l vs C_L)

Further information regarding wing parameters can be found in references [1] and [5].

2.2.5.4 Time dependence

All two coefficients are time-dependent, and the variation of the coefficients as time passes is a very important parameter to study the turbulent behavior of the flow. When flow becomes turbulent along most of the wing, c_l and c_d coefficients become cyclical and they oscillate following a certain pattern.

2.2.6 Stall

2.2.6.1 Definition

A stall is a condition in aerodynamics and aviation wherein the angle of attack increases beyond a certain point such that the lift begins to decrease. The angle at which this occurs is called the critical angle of attack. This critical angle is dependent upon the profile of the wing, its planform, its aspect ratio, and other factors, but is typically in the range of 8 to 20 degrees relative to the incoming wind for most subsonic airfoils. The critical angle of attack is the angle of attack on the lift coefficient versus angle-of-attack curve at which the maximum lift coefficient occurs.

Flow separation begins to occur at small angles of attack while attached flow over the wing is still dominant. As angle of attack increases, the separated regions on the top of the wing increase in size and hinder the wing's ability to create lift. At the critical angle of attack, separated flow is so dominant that further increases in angle of attack produce less lift and vastly more drag.

2.2.6.2 Stall speed

Stall speed is defined as the velocity of the aircraft when stall occurs. It has to be reminded that what causes stall is reaching the critical angle of attack. However, as it has been seen, the lift coefficient depends on the angle of attack.

$$C_L = f(\alpha)$$

Therefore the maximum lift coefficient uniquely depends on the critical angle of attack.

$$C_{L_{max}} = f(\alpha_{crit})$$

Thus the stall speed is computed as:

$$V_{stall} = \sqrt{\frac{2L}{\rho S C_{Lmax}}}$$

Stall speeds can then be compared for the same aircraft using the maximum lift coefficient - which depends on the critical angle of attack -, as long as air density and weight are kept the same for different tests.

A good summary of factors that influence the stall speed can be found in reference [6].

2.2.6.3 Stall detection

The criterion used to detect the stall in CFD will be set for every type of simulation, as a lot of factors influence the stall and a CFD simulation might not detect them all at once and detecting just some symptoms might be enough.

Symptoms that stall might be occurring can be the following:

- Increases in angle of attack do not result in an increase of lift.
- Increases in angle of attack do result in massive drag increases.
- Lift and drag coefficients become cyclical and do not have the same values over time due to high amount of turbulence over the wing.
- Flow is detached over a certain part of the wing profile – detached flow over about 15-30% of the chord length should be enough to call a stall.

2.2.7 Law of the wall

2.2.7.1 Parameter definition

Flow near walls can be divided into three different layers. An inner layer that is very close to the wall (viscous sublayer), an outer layer relatively far from the wall (defect layer) and a layer in between (log layer). As it has been exposed, the inner layer is dominated by viscous stresses and the outer layer is dominated by momentum transport due to Reynolds stresses. The parameter y+ is the non-dimensional wall normal distance defined as

$$y^+ = \frac{y u_t}{\nu}$$

and

$$u_t = \sqrt{\frac{\tau_w}{\rho}}$$

is the friction velocity, where

$$\nu = kinematic\ viscosity\ in\ m^2/s$$
$$\tau_w = wall\ shear\ stress\ in\ Pa$$
$$\rho = fluid's\ density in\ kg/m^3$$

And the non-dimensional velocity is also defined as:

$$u^+ = \frac{u}{u_\tau}$$

with

$$u = velocity\ parallel\ to\ the\ wall\ in\ m/s$$

2.2.7.2 Velocity profile for different y+

A velocity profile for a turbulent boundary layer like the ones that the study will encounter later on is illustrated in Figure 9.

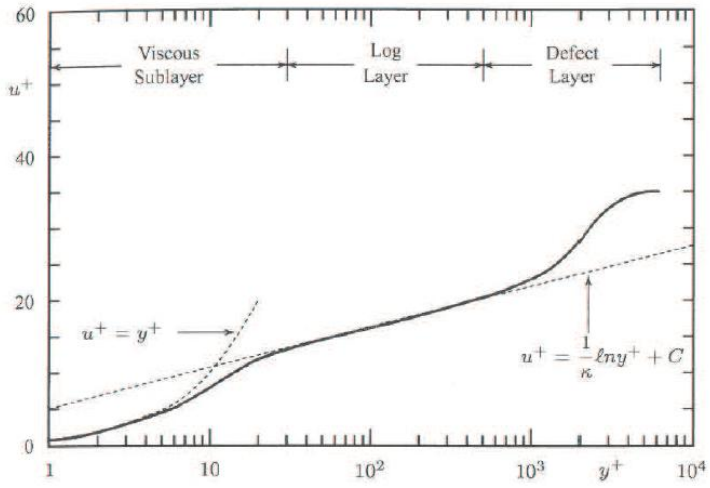

Figure 9: Typical velocity profile for a turbulent boundary layer. Source [7]

As the figure above graphically shows, for values of 1 < y+ < 5, the relation between velocity and distance to the wall is

$$u^+ = y^+$$

And for 30 < y+ < 500 the law of the wall is valid, which states that

$$u^+ = \frac{1}{\kappa} ln y^+ + C$$

However, this equation is valid until the upper limit of y+ which is usually 500. However, if Reynolds increases, the law of the wall equation is valid for higher y+.

values. The lower limit of y+ where the law of the wall is valid stays roughly the same for different Reynolds numbers.

The reason why all this is important in this study is because different turbulent models assume that the first layer of computational cells are either in the log layer or in the viscous layer. This assumption might be wrong as there is a transition region in between (defect layer) that doesn't correspond with any law of the wall, as it can be seen in Figure 9 ($5 < y+ < 30$).

Since the y+ values are dependent on flow characteristics they are not available during pre-processing. Therefore it is important to analyze the y+ values during post-processing in order to control that they correspond with the needs of the turbulent model, thus that they simulate an accurate boundary layer and all the effects present in it.

If y+ values do not correspond with the mesh sizing and the law of the wall that the solver is using to solve the equations, the boundary layer is not simulated properly. Therefore, results of simulations without VG might be inaccurate and results of simulations containing VG might not even reflect the physical effect of the devices.

2.2.7.3 Y+ wall distance estimation

The methodology to tackle this problem is to properly calculate the wall distance y, in other words: the mesh's first cell height. The minimum element size in the wall should always be smaller than the wall distance calculated for a desired y+. The minimum element size parameter must be calculated in order to create a proper mesh close to the wall, and this can be done automatically in CFD online pre-processors. [8]

However, it is important to know the relations behind this calculation and the steps followed, which can be found in the section 1 of the Annexes.

2.2.7.4 Law of the wall importance

The ideal situation to simulate a boundary layer would be the one where y+ could be set to y+=1 or less and generate a massive mesh that is able to create a velocity profile from the very first element. However, this might not be possible due to computational power limitations, so other options are also valid in CFD. Setting y+=100 would mean that the very first element of the grid would now be much bigger thus it would definitely not process the tiny viscous sublayer properly. However, by telling the solver that the first element attached to the wall follows a certain law of the wall, one can find a compromise solution between computational power and accuracy.

2.2.8 Turbulence modeling

2.2.8.1 Importance of turbulence modeling

This paper will not go through the theoretical principles of turbulence modeling. However, it is important to highlight the importance of choosing a good turbulence model to study any particular case of fluid dynamics.

In this case, it is important so simulate boundary layer and 3D vortex properly, as well as stall characteristics. If that happens, chances of obtaining reasonable results increase.

Complexity of different turbulence models may vary strongly, depending on the details one wants to observe and investigate. Turbulence could be thought of as instability of laminar flow that occurs at high Reynolds numbers. Such instabilities origin form interactions between non-linear inertial terms and viscous terms in Navier-Stokes equations. These interactions are rotational, fully time-dependent and fully three-dimensional. Rotational and three-dimensional interactions are mutually connected via vortex stretching, and this is not possible in two dimensional spaces. Therefore, no satisfactory two-dimensional approximations for turbulent phenomena are available, which is of course why this paper seeks to study the 3D case – which rapidly means facing computational processing problems from the start.

Moreover, turbulence is thought of as random process in time. No deterministic approach is possible, which makes it impossible to determine correlations between flow variables in advance of the fluid to begin to flow.

Another important aspect of turbulence is that vortex structures move along the flow. Their lifetime is very long and turbulent quantities cannot be specified as local. This means that upstream history of the flow has also a great importance.

The ideal turbulence model should introduce the minimum amount of complexity into the modeling equations, while capturing the essence of the relevant physics.

As there is not a universal turbulence model available - yet -, there are some turbulence models and options that suit better some cases than others. That, by the way, makes the area of CFD modeling very intriguing and also extremely economically attractive.

A selection of the most relevant models to flow separation across airfoils and wings is explained below. All of them are found in the software that will be used to carry out the simulations**: Ansys Fluent 14.5.**

2.2.8.2 Turbulence modeling approach

Main approaches to solve turbulent flows are summarized below.

Reynolds-Averaged Navier-Stokes (RANS) Models

- **Eddy-viscosity models (EVM)**

One assumes that the turbulent stress is proportional to the mean rate of strain. Furthermore eddy viscosity is derived from turbulent transport equations (usually k + one other quantity).

- **Non-linear eddy-viscosity models (NLEVM)**

Turbulent stress is modelled as a non-linear function of mean velocity gradients. Turbulent scales are determined by solving transport equations (usually k + one other quantity). Model is set to mimic response of turbulence to certain important types of strain.

- **Differential stress models (DSM)**

This category consists of Reynolds-stress transport models (RSTM) or second-order closure models (SOC). One is required to solve transport equations for all turbulent stresses.

Computation of fluctuating quantities

- **Large-eddy simulation (LES)**

One computes time-varying flow, but models sub-grid-scale motions.

- **Direct numerical simulation (DNS)**

No modeling whatsoever is applied. One is required to resolve the smallest scales of the flow as well.

Models computing fluctuation quantities resolve shorter length scales than models solving RANS equations, so they generally provide better results. However, they have a much greater computer power demand. [22] [27] [21]

Reference [3], officially published by Ansys, the most commonly used software to simulate in CFD, widely explains the theory behind every turbulence model and the applicable cases for every model.

2.2.8.3 Spalart-Allmaras model

[9] The Spalart-Allmaras model is a relatively simple one-equation model that solves a modeled transport equation for the kinematic eddy (turbulent) viscosity. This embodies a relatively new class of one-equation models in which it is not necessary to calculate a length scale related to the local shear layer thickness. The Spalart-Allmaras model was designed specifically for aerospace applications involving wall-bounded flows and has been shown to give good results for boundary layers subjected to adverse pressure gradients.

The Spalart-Allmaras model has been implemented to use wall functions when the mesh resolution is not sufficiently fine. This might make it the best choice

for relatively crude simulations on coarse meshes where accurate turbulent flow computations are not critical.

On a cautionary note, however, the Spalart-Allmaras model is still relatively new, and no claim is made regarding its suitability to all types of complex engineering flows. For instance, it cannot be relied on to predict the decay of homogeneous, isotropic turbulence. Furthermore, one-equation models are often criticized for their inability to rapidly accommodate changes in length scale, such as might be necessary when the flow changes abruptly from a wall-bounded to a free shear flow.

Regarding wall boundary conditions, if the mesh is fine enough to resolve the viscosity-dominated sublayer, the wallshear stress is obtained from the laminar stress-strain relationship. If the mesh is too coarse, it is assumed that the centroid of the wall-adjacent cell falls within the logarithmic region of the boundary layer.

This paper, however, indeed requires properly resolved turbulence in order to capture the effects of flow transition and flow separation, so this model is not ideal.

2.2.8.4 k-ε models

Standard k-ε model

This semi-empirical two-equation turbulence model is a model based on model transport equations for the turbulence kinetic energy and its dissipation rate. In the derivation of the k-ε model, the assumption is that the flow is fully turbulent, and the effects of molecular viscosity are negligible.

Pros

- Robust.
- Widely used despite the known limitations of the model.
- Easy to implement.
- Computationally cheap.
- Valid for fully turbulent flows only.
- Suitable for initial iterations, initial screening of alternative designs, and parametric studies.

Cons

- Performs poorly for complex flows involving severe pressure gradient, separation, and strong streamline curvature.
- Lack of sensitivity to adverse pressure gradients.
- Numerical stiffness when equations are integrated through the viscous sublayer which are treated with damping functions that have stability issues.

This model has a very good near-wall treatment, allowing the user to use standard wall functions, enhanced wall treatment or even user-defined wall functions.

As this study focuses on the transition from laminar to turbulent and flow detachment, assuming that the flow is fully turbulent does not seem ideal.

RNG and Realizable k-ε model

[3] the RNG model was derived using a statistical technique. It is based in the k-ε standard model, but includes some refinements widely explained in the reference [3]. The Realizable model contains an alternative formulation of the turbulent viscosity. The term "realizable" means that the model satisfies certain mathematical constraints on the Reynolds stresses, consistent with the physics flows.

These features make the model more accurate and reliable for a wider class of flows than the standard k-ε model. However, refinements implemented are not useful for the study flow detachment over a wing.

2.2.8.5 Standard and SST k-ω models

Standard k-ω model

The standard k-ω model is an empirical model based on model transport equations for the turbulence kinetic energy and the specific dissipation rate. It incorporates modifications for low-Reynolds-number effects, compressibility, and shear flow spreading.

This model performs significantly better under adverse pressure gradient conditions. The model does not employ damping functions and has straightforward Dirichlet boundary conditions, which leads to significant advantages in numerical stability. This model underpredicts the amount of separation for severe adverse pressure gradient flows.

Pros:

- Superior performance for wall-bounded boundary layer, free shear, and low Reynolds number flows.
- Suitable for complex boundary layer flows under adverse pressure gradient and separation (external aerodynamics and turbomachinery).
- It can be used for transitional flows.

Cons:

- Separation is typically predicted to be excessive and early.
- Requires mesh resolution near the wall.

Regarding wall boundary conditions, enhanced wall treatments are used, which means that all boundary conditions for wall-functions meshes will correspond to the wall function approach.

Shear-Stress Transport (SST) k-ω Model

This model was developed to effectively blend the robust and accurate formulation of the k-ω model in the near-wall region with the free-stream independence of the k-ε model in the far field.

The new features make the SST k-ω model accurate and reliable for a wider class of flows, like adverse pressure gradient flows and airfoils.

Pros:

- Offers similar benefits as standard k–ω.
- The SST model accounts for the transport of turbulent shear stress and gives highly accurate predictions of the onset and the amount of flow separation under adverse pressure gradients.
- SST is recommended for high accuracy boundary layer simulations.

Cons:

- Dependency on wall distance makes this less suitable for free shear flows compared to standard k-w.
- Requires mesh resolution near the wall.

A Reynolds Stress model may be more appropriate for flows with sudden changes in strain rate or rotating flows while the SST model may be more appropriate for separated flows.

According to the pros mentioned above and bibliography that has worked with this models, this looks like a very appropriate turbulence model to simulate the aerodynamic effects concerning this paper. [10]

2.2.8.6 K-kl-ω transition model

This model is used to predict boundary layer development and calculate transition onset. This model can be used to effectively address the transition of the boundary layer from a laminar to a turbulent regime. No bibliography has been found using this model, although it looks appropriate for the simulations to be carried in this paper.

2.2.8.7 Transition SST Model

The transition SST model is based on the coupling of the SST k-ω transport equations with two other transport equations, one for the intermittency and one for the transition onset criteria, in terms of momentum-thickness Reynolds number. The model then has four equations.

This model does not use wall functions, so y+~1 is recommended although not necessary. This seems to be to most appropriate turbulence model to simulate transitional flow and detachment related phenomena [2], but the slowest convergence in comparison with the SST k-ω model –which should already give good results - might not be worth the extra computational power needed. However, for 3D simulations while using the Transition SST , using a proper y+ value is crucial

to obtain reliable results, and this translates into more computational resources needed when using this model.

2.3 VG aerodynamic behavior

2.3.1 VGs operating principle: boundary layer control

2.3.1.1 Qualitative approach

Boundary layer separation is clearly an unwanted phenomenon in most aerodynamic designs. When separation occurs it leads to loss of lift, higher drag and results in energy losses. This extreme situation is called stall.

A vortex generator is placed in a determined position of the extrados of a wing, inside the boundary layer. Each VG creates a pencil-thin tornado-like cone of swirling air that stimulates and organizes the turbulent flow of the boundary layer on the aft portion of the wing. The swirl of the vortices pulls fast-moving air down through the boundary layer into close proximity to the wing surface, energizing the previously dead air there.

In other words, the vortex interacts with the boundary layer air on the aircraft surface behind the device by inducing high-energy air from outside the boundary layer down to the surface displacing low energy air.

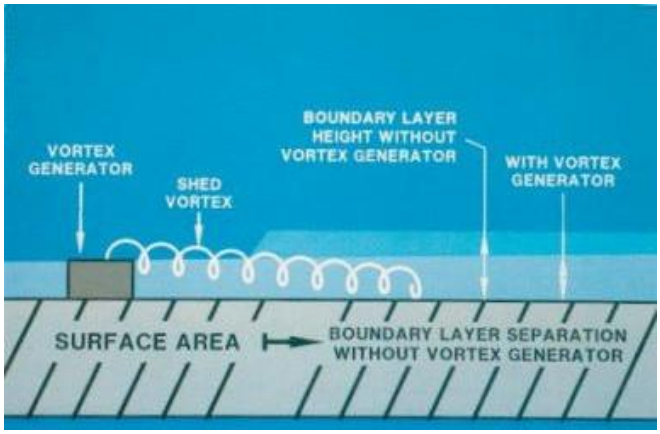

Figure 10: Vortex generator operating principle. Source [11]**.**

To summarize the basic effect caused by VGs, Figure 11 shows how, for a given angle of attack, flow remains attached when a proper configuration of VGs is being used, whereas the wing stalls if VGs are not implemented.

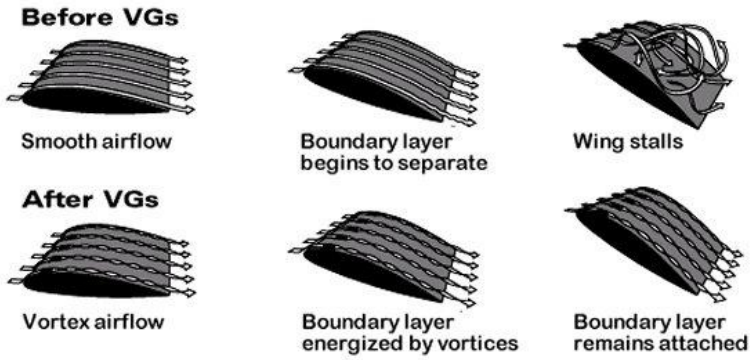

Figure 11: Qualitative drawing for different finite wings with angles of attack with and without VGs

Further information regarding the detailed study of the aerodynamic behavior of a single vortex generated by VG can be found in reference [10].

2.3.1.2 Numerical approach

According to the previous section, VGs basically boost the C_{Lmax} of the wing by contributing to attach the flow for higher angles of attack - see Figure 12.

Therefore, assuming

- Same aircraft model
- Equal air conditions
- Same flight conditions, where lift equals weight (L=W)

$$C_{Lmax_{VG}} > C_{Lmax_{clean}}$$

$$V_{stall_{VG}} < V_{stall_{clean}}$$

$$\sqrt{\frac{2W}{\rho S C_{Lmax_{VG}}}} < \sqrt{\frac{2W}{\rho S C_{Lmax_{clean}}}}$$

It is also numerically proven that stall speed for an aircraft using VGs is lower than without VGs.

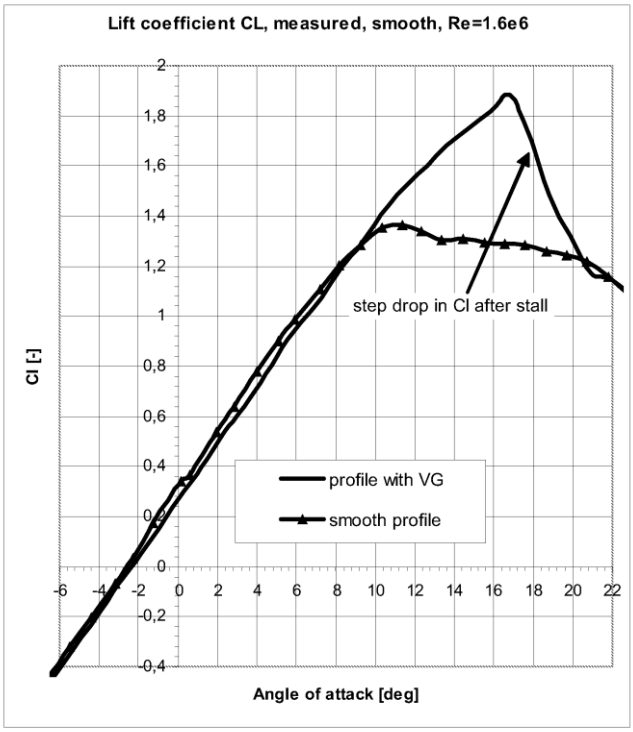

Figure 12: Lift coefficient comparison between clean and VG configurations. Source [12].

2.3.2 Dimensions and configurations

The study of positions, dimensions and characteristics of different VG configurations is complex and has to take into account a lot of factors and parameters.

The variables to be studied in the implementation of vortex generators are the ones seen in the Figure 13: angle of incidence, height and length of the device, the relative position between VG couples and the relative distance between VGs in a couple.

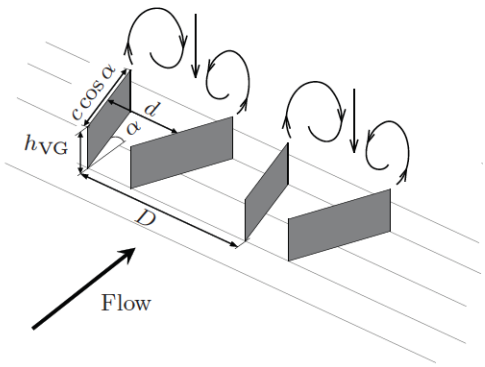

Figure 13: Close-up scheme of two pairs of VGs and its characteristic parameters. Source [13].

Different shapes of VGs exist, as it can be seen in Figure 14, but triangular and ogive shapes are the most common in general aviation.

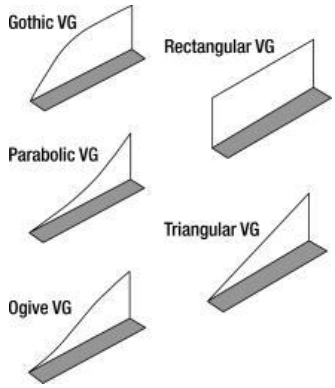

Figure 14: Different shapes of the state of the art VGs. Source [13]

References [10] and [14] feature very accurate studies regarding different VGs configurations, while reference [2] explains a lot of physical effects on vortex themselves. VGs used for simulations and experimental tests in this paper will follow those documents as a reference to proceed.

2.3.3 Advantages and downsides of VG

The use of VGs in ultralight aircraft has a good number of advantages but also some downsides that need to be considered and thus minimized with the implementation of such devices. [15]

Benefits

- **Lift coefficient increase at high angles of attack:** causing a similar effect as deploying flaps, VGs implementation increases the maximum c_l. It prolongs the lift coefficient vs angle of attack due to a later flow separation from the wing.
- **Stall speed reductions:** as a consequence, stall speeds (Vs) are drastically reduced. Depending on the type of airplane, stall speed reductions range from four to ten knots.
- **Increased aileron authority:** along with the reduction in stall speed, VGs give an increased maneuverability to the ultralight by not allowing the detachment of boundary layer of the control surface at low speeds.
- **Better aerodynamic behavior at low speeds:** consequence of the previous advantage, aircraft using vortex generators behave better in near-stall conditions, thus it helps dealing with emergencies and abnormal situations.
- **Minimum control speed (Vmc) reduction:** as a consequence, when the airflow remains attached at lower speeds and the control surfaces

are effective at lower speeds, the minimum velocity at which the aircraft is maneuverable decreases.

- **Take-off distance reduction:** as a consequence of the previous advantage, the aircraft can lift-off at an earlier velocity during its take-off roll.
- **Landing distance reduction:** as the stall speed is reduced, the ultralight can approach and land at lower speeds, as approach and landing speeds are usually the product of the stall speed by a certain security parameter. If the plane lands at lower speeds, it is easier for the pilot to stop the aircraft.
- **Steeper climbs:** as a direct consequence of the maximum lift coefficient increase, the aircraft performance improves and steeper climbs can be executed.
- **Gross weight and landing weight increase and:** this benefit applies to general aviation mainly, as for ultralight aircraft the 450kg weight restriction makes that these aircraft are often not fully loaded thus not being used inside their limits. More information about this benefit has been summarized in the section 2 of the Annex.
- **Inexpensive and easy way to improve aircraft performance:** as it will be seen in the next section, vortex generators kits are neither expensive nor difficult to mount on an aircraft wing. They produce better effects than slats and they can be added to any aircraft wing – as long as it is properly certified by the aircraft builder.

Downsides

- **Drag creation:** even that VGs surface normal to the aircraft velocity is almost negligible, there is an additional drag creation associated with VGs implementation.
- **Cruise speed reduction:** due to additional drag creation, some aircrafts suffer a slight cruise speed reduction of about 1-3 knots.
- **Icing:** VGs are usually sized to a height of about 80% of the boundary layer thickness, but if they are tall enough as to poke up through the boundary layer and they are abnormally situated too close to the leading edge, VGs could pick up ice. This is a rare situation and no reports or experiences regarding this have been found.
- **Abrupt stall behavior if used incorrectly:** most of the aircraft that use vortex generators detect a later, smoother and more controlled stall. However, a poor use of vortex generators – wrong configurations, design or implementation – can lead to nasty stall characteristics.

Various real testimonials with very interesting feedback from the installation of VGs can be found online in references [15], [16] and [17].

2.3.4 VG State of the Art in ultralight aircraft

2.3.4.1 Applications

Applications for vortex generators in ultralight aviation may vary depending on where of the aircraft the vortex generator is placed, thus the main places where vortex generators are used are described below.

Wings

The main use of vortex generators is to delay flow detachment on wings to improve stall characteristics, so the greatest influence on the effectiveness of vortex generators is their location on the wing.

If they are placed too far away from the leading edge, their performance during the stall will be negligible. This is due to the boundary layer, and the separation. If vortex generators are placed too close to the leading edge, it can cause increased drag. It's better to mount farther forward than too far aft leading edge. The permissible range is considered to be 6-10% of wing chord back from the leading edge to the front of vortex generator.

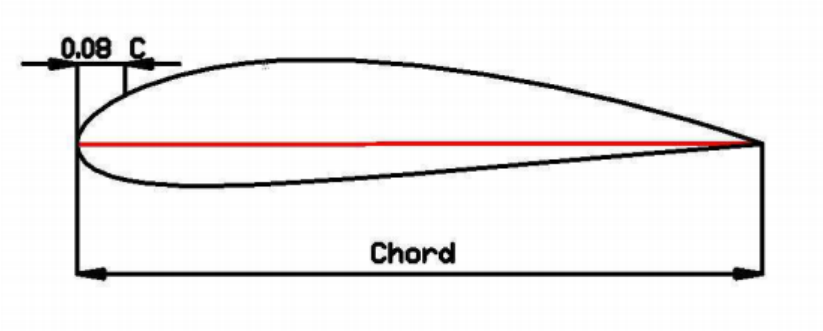

Figure 15: Schematic position of the typical position of vortex generators

Figure 16: Vortex generators devices mounted along an ultralight wing.

Control surfaces

Vortex generators are often placed on horizontal and vertical stabilizers to benefit from the increase in maneuverability. This is a very common practice in gliders, where control surfaces are even more critical.

Nacelles

This applies to general aviation only, as ultralight aircraft are not multi-engine. Most of the twin-engine kits also come with a pair of nacelle strakes that act like large VGs for the wing-to-nacelle interface. The nacelle strakes create a large vortex that acts like a stall fence and prevents the stall from propagating outboard of the nacelles. [16]

Figure 17: Nacelle vortex generator mounted on a multi-engine airplane. Source [16]**.**

2.3.4.2 Distributors

There are plenty of reliable distributors for official VG kits. Beryl D'Shannon, Boundary Layer Research, RAM aircraft and most popularly, Micro Aerodynamics are the main official distributors of VG kits for general aviation in the US.

In Spain, as most of the aviation that uses this kind of device is experimental, kits are obtained online and there is no specific main distributor in the country.

2.3.4.3 Cost

As for experimental aviation, prices for a VG kit vary between 90€ and 250€, without computing the cost to mount them into the aircraft. Vortex generators can also be built by oneself with an aluminum plate and the proper tools, but this will be discussed and explained in the last chapter of the paper.

There is also data available for approximate costs of VG kits for certified single engine aircraft. Prices for a complete VG kit vary widely from 600€ to 1300€. Prices are higher because of the cost of the certification of the devices. Further discussion regarding this topic can be found in the section 3 of the Annexes.

2.3.4.4 Installation

VG manufacturers always want to remind that vortex generators will not fix incorrectly flying aircraft, wrong balanced, or having inadequate geometry.

A VG kit includes everything needed for installation. There are peel-and-stick templates to put at defined locations. The skin is roughed up at each VG-to-be spot and each VG is glued in place.

References [16] and [18] have very clear instructions and interesting experiences regarding VG kits installation, respectively

2.4 Ultralight model choice

The ultralight brand and model chosen for this study is an **Alto TG 912 ULS.**

2.4.1 Choice justification

The reason for this choice is that - in the likely event of having the resources and time to perform flight tests - the author of this project is enabled to pilot this ultralight model, as he possesses an ultralight pilot license since 17-01-2013. This aircraft can be found in Igualada - Ódena (LEIG) aerodrome in the *Aeronautico 2000* club, where the author belongs.

The author usually pilots a Tecnam P96 Golf ultralight, a more conventional, older and lower performance small aircraft. However, the reason to choose the Alto is that it is flying under an experimental aircraft license (see section 5 of the Annexes), which allows amateur built ultralight to fly in certain circumstances and airspace with any minor modifications that the airplane's constructor (club's head and founder) considers reasonable. VGs are indeed considered a minor change to the aircraft (in fact, it's a common practice to add them to ultralight aircraft) so flight tests for this study would be fine according to this legislation. It might be fine doing this with other ultralight models such as Tecnam as well, but for this occasion the Alto model has been chosen.

2.4.2 Brief description

According to its builder, the Alto aircraft is a simple, all-metal construction useful also for amateur working conditions. The Alto has adequate power corresponding to standards of this category with low maintenance costs and with simple and friendly control in flight.

The ALTO aircraft meets both requirements to European category "ultralight aircraft" and requirements to "light sport aircraft" (LSA) category that has been defined in the U.S.A. The configuration of this model includes:

- Tricycle, nose type landing gear
- Engine ROTAX 912 ULS - 100 Hp
- Dual stick control

2.4.3 Charts

The builder provides a good number of plans to allow the construction of the aircraft. The main plan of the original aircraft that has been used can be found in the section 4 of the Annexes.

2.4.4 Relevant dimensions and performances

Relevant data and performances to take into account for this study, given by the builder [19] [20], can be found in the following table:

RELEVANT DATA	ALTO TG 912 ULS
length	6.15m
mean aerodynamic chord	1.315m
wing span	8,2m
fuel	110 litres
empty weight	288kg
MTOW - ULM	450kg
cruising speed	200 km/h
Stall speed flaps up	75 km/h
Stall speed full flap	62 km/h
Take-off roll distance (grass)	120m
Take-off roll distance (pav)	110m
Landing roll distance	91m

Table 1: Relevant manufacturer data for the ultralight model Alto TG 912 ULS. Sources [19][20].

Take-off and landing distances will not be used to contrast data, but they can be really useful for further studies on the impact of VGs on landing distances.

2.4.5 Airfoil

According to the chart provided by the aircraft builder, this ultralight uses a NACA 3415 airfoil, which is represented below:

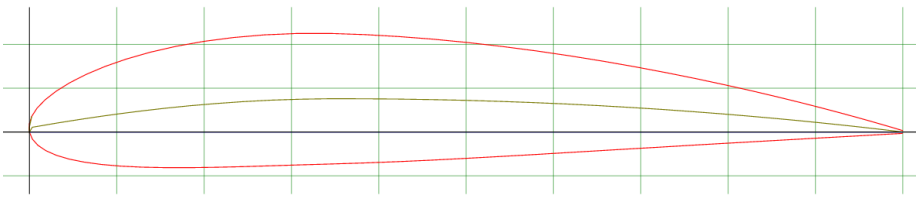

Figure 18: NACA3415 airfoil plot

2.4.6 Other aspects

Relevant to the aerodynamics, it can be seen that:

- Wings have no swept angle.
- Dihedral angle is 3.5 degrees.

- The wing consists in an extrusion of the airfoil from the root to 20cm before the tip, where some torsion is added to create a winglet shape.

In next chapters it will be discussed if those characteristics are relevant or not for the aerodynamic simulations.

PART III: SIMULATION

3.1 Aim of the simulation stage

The aim of the first simulation stage – the one that is carried out in this paper- will be setting an accurate criterion and work on the previous steps to achieve the second stage aim. Discussing 2D and 3D results and contrasting them with experimental data found in this paper should allow a second round of work to tackle the final aim of the whole simulation stage.

The software to be used for the simulations will be **Ansys Fluent 14.5**, which contains the broad physical modeling capabilities needed to model flow and turbulence.

In general, as this paper has some limitations that have been mentioned above, the ideal scenario will be exposed but in some cases power limitations will not allow the study to accomplish with the ideal standards. This is why ideal conditions will be mentioned and then results obtained with affordable scenarios will be cautiously analyzed. The aim of the study is to set a criterion to distinguish between valid grids, models, and data introduction and to be able to analyze the results accordingly.

Below is exposed the aim of the second simulation stage, which will not be carried out in this paper.

Aim of the second simulation stage

The final aim of a professional simulation stage could be analyzing the effects of the implementation of different VGs configurations in a wing of an ultralight aircraft in order to determine the best option among all the VG available configurations for the given aircraft. The best option would be the one with a better overall performance, which will be seen as a compromise solution between different parameters such as:

- Best Stall speed reduction
- Minimum drag creation
- Lowest cost ($) of the device / difficulty to build it

As mentioned, details of the preliminary simulation stage are exposed in the rest of part III of the paper.

3.2 2D airfoil simulation

3.2.1 Computational power limitations

A 16GB RAM machine and 3,1GHz i7 processor were used to carry out the simulations.

To have a rough idea of the computational cost of the simulations performed, every 2D simulation took around 30-60 minutes to simulate around 4-5 seconds of flow time.

As angle of attack of the flow was increased the time of computation increased too, as the equations took way more time to converge. Apparently, the reason for this is that more turbulence is generated for higher angles of attack thus slowest convergence was to happen as laminar flows are easier to solve than turbulent ones.

In the section 11 of the annexes, more information regarding solution convergence can be found.

3.2.2 Geometry modeling

Some previous steps are needed in order to choose and create the geometries that will be introduced to the simulation software.

3.2.2.1 Airfoil identification

As there was no information available regarding the exact airfoil that the aircraft is using, it was properly identified from the charts given by the builder. Using Photoshop, the three parameters that define a NACA four-digit series airfoil were found:

- Maximum camber as percentage of the chord: **3.8%**
- Distance of maximum camber from the airfoil leading edge in tens of percents of the chord: **35%**
- Maximum thickness of the airfoil as percent of the chord: **15%**

Thus the airfoil used for the simulations will be NACA 3415.

3.2.2.2 Airfoil data pre-processing

To create geometry to be analyzed in Fluent, consisting on an airfoil and the possibility to efficiently add or remove different types of VG, the author chose to use **Solid Works.**

3.2.2.3 Domain definition

Although the domain definition is strictly related with the mesh criteria which will be discussed later, the geometry creation itself is done at this stage of the project.

In 2D, the ideal conditions can almost be achieved in this paper. An empty space called control volume around the airfoil where air will freely flow is generated. This space has to be big enough as to avoid interactions between the fluid and walls of the control volume. Cornell University fluent tutorials [21] proposes what is usually called a C-domain for a 2D airfoil analysis.

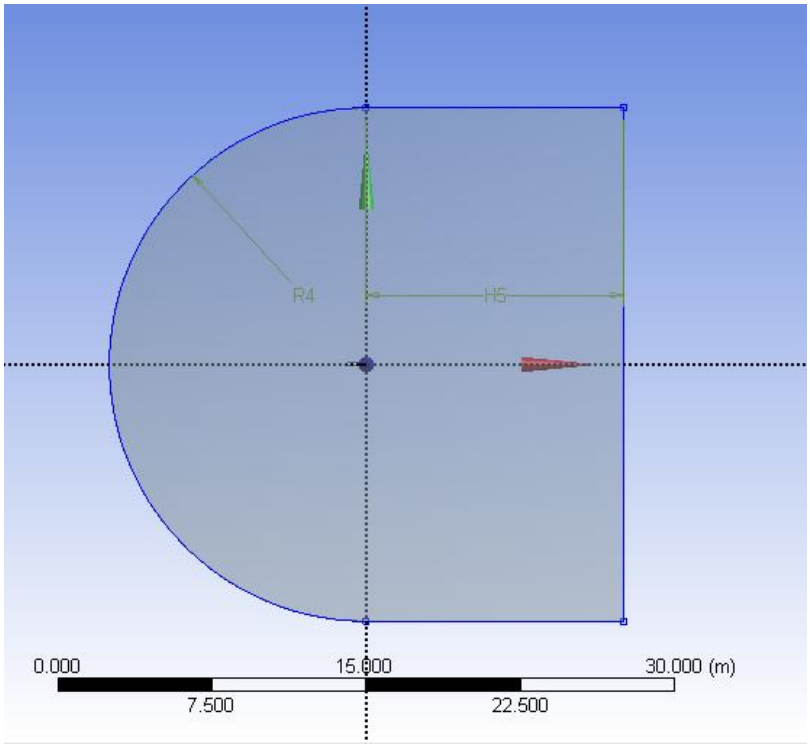

Figure 19: C-domain used for 2D airfoil simulations

Assuming a chord length c of 1m, as it will be later scaled inside Fluent software, distances between the airfoil and the control volume walls are, according to the Figure 19.

R4 = 12.5c

H5 = 12.5c

3.2.3 Simulation criteria

This section clearly exposes the criteria chosen by the author to carry out the simulations. It also tries to argue the process that a deeper study should follow in order to optimize the simulations and obtain more reliable results. However, note that even the 2D part of the simulation is being used as a previous step to obtain reasonable results, validate them, and compare them with 3D simulations, this paper tries to stay methodic and cautious, as it is a big mistake to automatically trust this kind of simulation results taking into account the project's academic limitations. Therefore, more than trying to obtain very accurate results, the simulation criteria and results verification steps are taken very seriously, so the study could follow a correct path to more professional and commercially applicable results.

3.2.3.1 Turbulence model preference

Fluent offers the possibility to use a wide range of models to solve the finite element problem. Each of them has been deeply studied in section 2.2.8 and they have their pros and their cons, although only one of them should be ideal to simulate VGs' effects.

After a lot of tests and bibliography consulting, the **Transition SST 4 equations turbulence model** was chosen as it was good at predicting flow separation in 2D and it was also proved by bibliography [2].

Note that this is an iterative process where the whole simulate stage has to be carried out numerous times in order to establish a reasonable turbulence model preference. Note that turbulence model choice is related to y+ calculation and mesh refinement, so the process gets rather complex.

3.2.3.2 Y+

As it has been discussed before, the y+ is an important parameter in CFD simulations in order to calculate the first cell height and properly simulate the boundary layer and the conditions near the airfoil.

Ideal y+

To accurately simulate the boundary layer and its detachment with the Transition SST turbulence model, y+<1 would be ideal [9].

As it has been mentioned, the first cell height calculator would need the following input data:

INPUT	Ideal situation data
Freestream velocity	35 m/s
Fluid density	1.225 kg/m^3
Fluid dynamic viscosity	1.7894·10-5 kg/ms
boundary layer length	1.315m
desired y+ value	1

Table 2: input data for the ideal 2D analysis situation

Freestream velocity is 126 km/h, which is the speed used for climb, patterns and maneuvers. It is also the best gliding speed, according to the aircraft's user manual [19]. This ultralight usually deploys flaps at 120km/h to perform the approach.

Note that the geometry has a chord length of 1m, but in Fluent the geometry can be scaled and the chord length increased to 1.315m, which is the real dimension. Standard air conditions have been chosen too.

OUTPUT	ideal data
Reynolds number	$3.2 \cdot 10^{6}$
Estimated wall distance	$1.1 \cdot 10^{-5}$m

Table 3: Output estimated wall distance for the ideal 2D analysis situation

Affordable y+

This turbulence model uses automatic wall functions which would solve this inaccuracy, but it is still highly recommended to simulate the entire viscous sublayer for better performance.

However, due to computational power limitations, author used **y+=30**

INPUT	affordable analysis data
Freestream velocity	35 m/s
Fluid density	1.225 kg/m^3
Fluid dynamic viscosity	1.7894·10-5 kg/ms
boundary layer length	1.315m
desired y+ value	30

Table 4: input data for the affordable 2D analysis situation

OUTPUT	Affordable data
Reynolds number	$3.2 \cdot 10^{6}$
Estimated wall distance	$3.2 \cdot 10^{-4}$m

Table 5: output estimated wall distance for the affordable 2D analysis situation

According to this y+ calculation, the chosen mesh criterion is exposed below.

3.2.3.3 Mesh

Ideal mesh

An ideal situation would mean being able to create and compute a mesh that met the following requirements:

- y+=1
- 15-30 layers refinement on the boundary layer
- Enough refinement in the leading and trailing edge
- Enough refinement in the downstream flow over the airfoil – the "back of the airfoil".

Additionally, in meshing there are some parameters that help to identify good or bad quality grids: skewness and element quality - see [22].

The conceptual procedure that should be followed to create a proper grid is illustrated in the section 8 of the annexes and is further developed in reference [23].

Numerically, the NACA 3415 airfoil grid concerning this paper should meet

2D ideal mesh	
elements	>50.000
first cell height	$1.1 \cdot 10^{-5}$m
max skewness	<0.25
min orthogonal quality	>0.80

Table 6: Ideal mesh characteristics for a 2D airfoil analysis

Moreover, the ideal software to create grids around airfoils and wings is ANSYS ICEM CFD, which is one more complex software that allows the user to create high quality grids around complex geometries and refining them where necessary with the help of a previous tedious sketching of H, O or C geometries – see [23].

Nice looking accurate meshes like Figure 20 and Figure 21 can be generated.

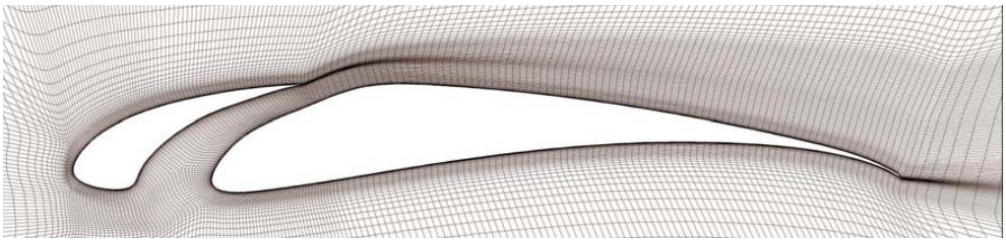

Figure 20: ICEM good quality generated mesh for a given airfoil with a slat. Source [24]**.**

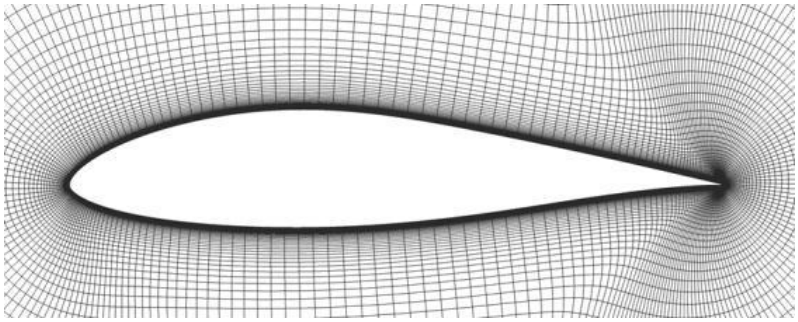

Figure 21: ICEM good quality generated mesh for a given airfoil. Source [25]

Boundary layer and specially trailing edge should be refined with care to increase accuracy of the simulations. Figure 22 perfectly describes how to successfully refine the trailing edge.

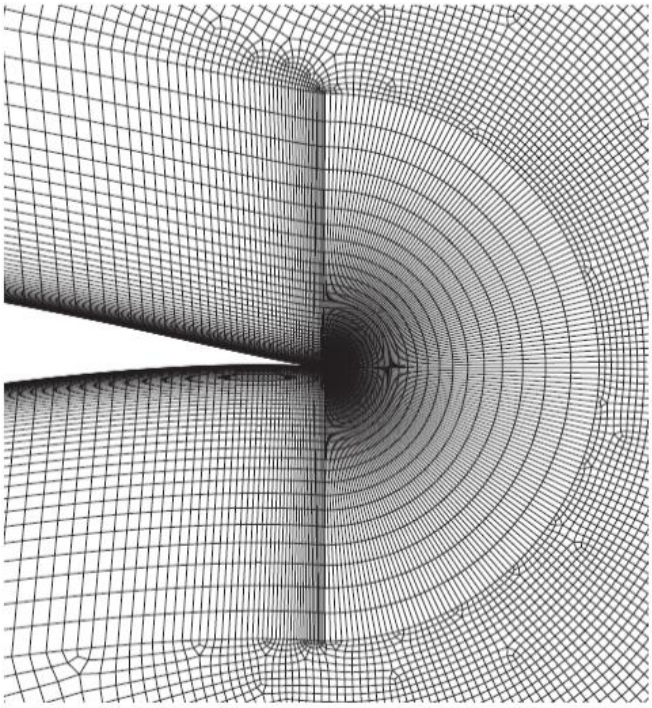

Figure 22: View of grid near trailing edge of S809 airfoil. Source [2]**.**

Affordable mesh

According to the project's possibilities, a well refined mesh was created around the airfoil thus it is not properly optimized. The high amount of elements could be distributed in a different way around the control volume in order to increase the mesh quality and optimize the results. This mesh was giving very reasonable and even good results after some preliminar testing, so it was decided not to change it.

The procedure followed to generate the mesh, based on a Cornell University tutorial, was the following:

- C-type unstructured mesh refined on a radius of 3m around the airfoil with 0,03m elements

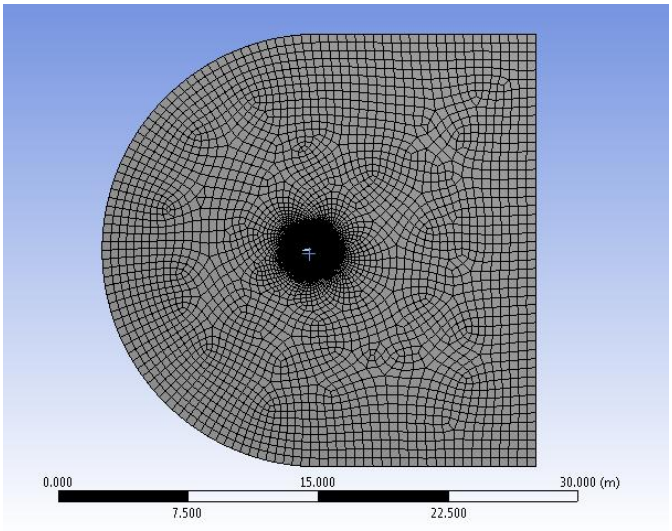

Figure 23: C-mesh used in 2D simulations overview

- Second refinement with smaller element sizing on a radius of 0.5m around the airfoil with $8 \cdot 10^{-4}$m elements.
- Edge sizing of 450 elements around the airfoil.

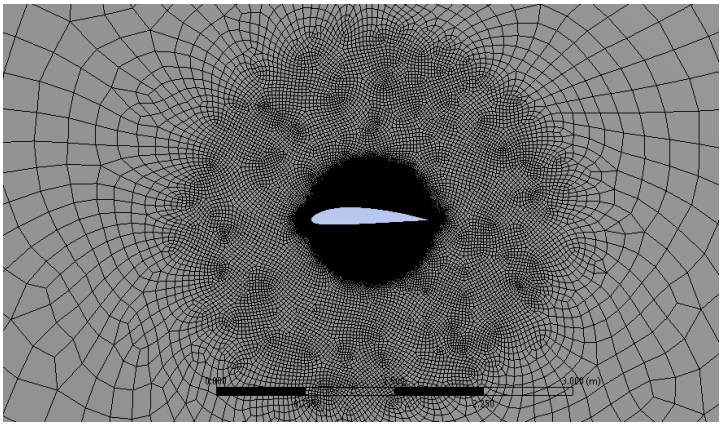

Figure 24: Mesh around airfoil used in 2D simulations zoom view 1

- Third refinement in the leading and trailing edge with $5 \cdot 10^{-4}$m elements.

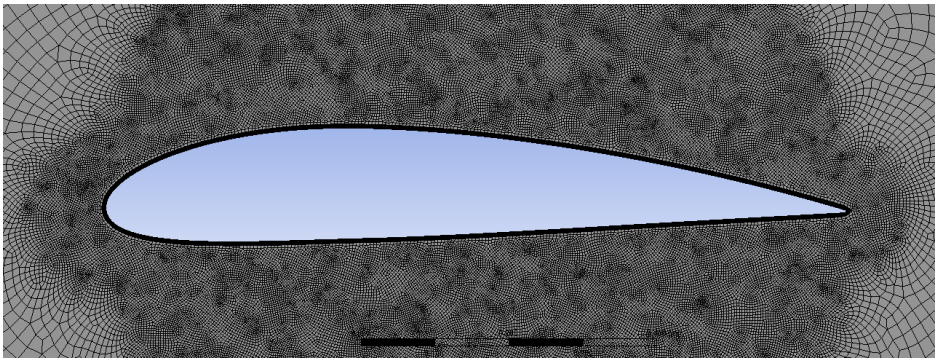

Figure 25: Mesh around airfoil used in 2D simulations zoom view 2

- Element inflation in the airfoil edge in order to simulate a good boundary layer that meets the requirements and law of the wall for the desired y+. First cell height was $3 \cdot 10^{-4}$m, 14 layers with a growth rate of 1.08.

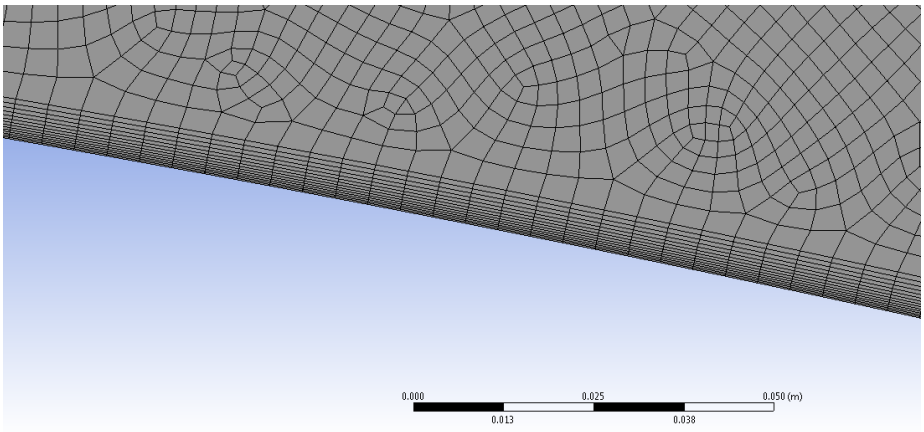

Figure 26: Mesh around airfoil used in 2D simulations zoom view 3

The mesh used for the 2D simulation has the following characteristics:

2D affordable mesh	
elements	99729
first cell height	$3 \cdot 10^{-5}$m
average skewness	0,14
max skewness	0,86
average orthogonal quality	0,978
min orthogonal quality	0,222

Table 7: Mesh characteristics used in 2D simulations

These parameters are not optimal, as defining the refinement with a circumference is not ideal, but the mesh has delivered good results.

3.2.3.4 Grid independence

Results have to be checked not to be dependent with mesh characteristics, evidently to a certain extent, as very coarse meshes deliver poor results. This is a mandatory verification in CFD simulation, as grid dependent results are totally unreliable.

As the grid creation is an iterative process, the grid was tried to be refined but changes in final results were not noticeable. Making the grid coarser delivered poorer lift predictions and inaccurate stall and flow detachment conditions.

3.2.3.5 Time step

As simulations are intended to study flow separation and turbulence, which are rather over-time phenomenon, the transient analysis is a must. Time step used for non-steady simulations has to accomplish a very simple condition: not allowing a fluid particle go through more than one cell for the given time step. This means that the maximum velocity of the fluid cannot be higher than the minimum cell axial length divided by the time step. This can affect results accuracy and solution's convergence.

This is actually computed by the Courant nondimensional number, defined as:

$$C = \frac{\Delta t}{\frac{\Delta x}{u}} \leq 1$$

After some grid scanning and some previous simulations, the minimum cell length in the x axis is $\Delta x = 8 \cdot 10^{-4} m$ and the highest velocity achieved by the fluid (found in the leading edge) is u=56.5 m/s, therefore the maximum time step can be computed as:

$$\Delta t \geq \frac{u}{\Delta x} \geq 1.456 \cdot 10^{-5} s$$

However, transient analysis were carried out for time steps of this order of magnitude and then Δt was increased to check if results were dependent or not of it. For Δt>0.01s some cyclical lift coefficients caused by oscillations near the stall began to not be captured properly, thus for computer-time-saving the time step used to carry out the transient 2D simulations is **Δt=0.005s.**

3.2.3.6 Stall detection

The criterion set for stall detection in the simulations will be a combination of the factors mentioned in the theory study.

- Lift decrease or stagnation with angle of attack increase.
- Noticeable flow detachment over the airfoil.
- Lift and / or drag oscillating coefficients over time.

Ideally, if the mesh and turbulence models allowed the simulation to be as optimal as possible, detecting the critical angle of attack should be enough to detect stall. However, airfoil stalls and post-stall conditions are already a source of big CFD problems, as the author has been able to confirm with the bibliography and surfing CFD forums. There are even some studies that focus only on stall detection and post-stall situations, like reference [26].

Therefore, post-processing the simulation and taking a look to the velocity vectors and checking for oscillations on forces over the airfoil, which would mean

turbulence presence, should be good to help detect stalls. As the analysis is obviously transient, the lift and drag coefficients will be monitored in Fluent to detect cyclical values.

3.2.4 Simulation results and discussion

This section exposes the results obtained during simulations, which have been accurately carried out according to the criteria exposed above.

For a qualitative analysis, some contours and velocity streamlines were plotted for three different angles of attack. At 15º of AoA the airfoil should be in a stall condition according to experimental data [27].

Blue regions stand for low pressure zones while red / orange regions correspond to high pressure values. As it can be seen in Figure 26, the simulation predicts well the suction in the extrados of the airfoil and the increase of pressure difference between surfaces.

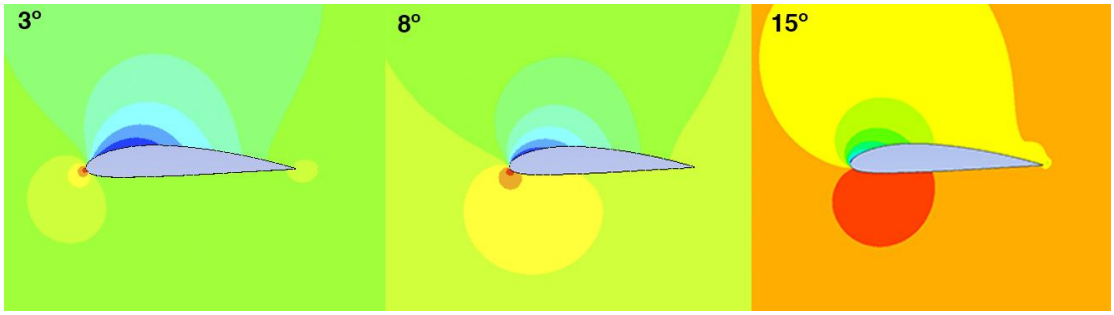

Figure 27: Pressure contour plot of the affordable mesh 2D analysis at 3 different AoA. Blue is for low pressure while red colors are for high pressure.

By plotting the velocity contours – blue stands for low flow velocities and red stands for highest velocities – one can appreciate the increase in the difference of velocity between surfaces. In the 15º angle of attack plot it seems clear that the airfoil is under stall condition as almost a 40% of the extrados flow is detached. This can be seen in the blue region, which means that flow has almost zero velocity and even negative values in the component of free-stream velocity.

Note how for angle of attack 8º the velocity contour colors change a little too sudden from yellow to light green in the upper part of the plot. This might be due to a wrong convergence of the equations of the elements around that zone, a too coarse mesh or a too big time step. However, this particularity does not seem to affect overall results.

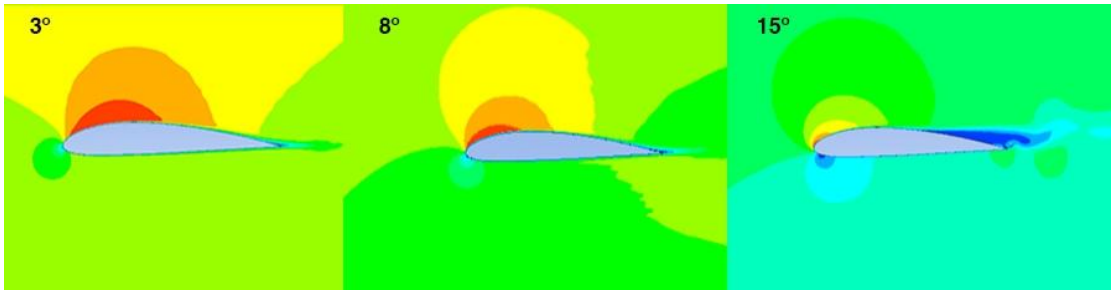

Figure 28: Velocity contour plot of the affordable mesh 2D analysis at 3 different AoA. Blue is for low velocities while red colors are for high velocities.

Figure 29 shows the velocity streamlines around the airfoil. It is a great tool to appreciate the increase in the angle of attack and the adverse pressure gradient that is generated in the 15º angle of attack plot; there is one streamline that turns against free-stream velocity direction and after some vortex it rejoins the flow again. This confirms in a more graphical way the detachment of the boundary layer in the trailing edge and evidences turbulence presence in that region.

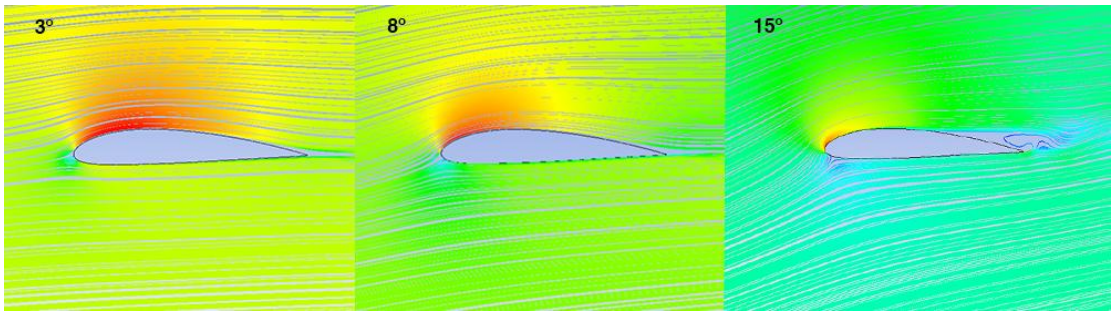

Figure 29: Velocity streamlines of the affordable mesh 2D analysis at 3 different AoA. Blue is for low velocities while red colors are for high velocities.

As this study focuses on flow separation and stalls detecting, a velocity contour of the airfoil under angles of attack close to the critical angle of attack has been plotted. The stall progression can be easily detected as the angle of attack reaches the critical value. For AoA=14º, it can be considered that the airfoil is in stall condition as a 30% of the extrados flow is detached. In the AoA=15º plot, it can be seen how turbulent and unstable the flow becomes in the trailing edge due to the detachment.

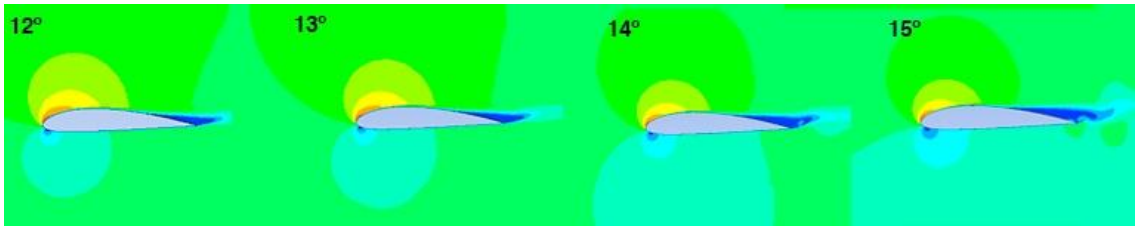

Figure 30: Velocity contour plot of the stall progression in the 2D analysis. Blue is for low velocities while red colors are for high velocities.

Reports of mean forces over the airfoil have been gathered. Forces have been projected in the wind-relative reference system and lift and drag coefficients have been calculated according to the theory exposed in previous sections.

Results delivered by the simulation look very reasonable as the range of cl from AoA=0º to 14º looks lineal. Then the critical angle of attack (15º) is reached and lift begins to decrease.

So far, flow post-processed results and lift coefficient curve seem to agree that the critical angle of attack should be around 14º-15º.

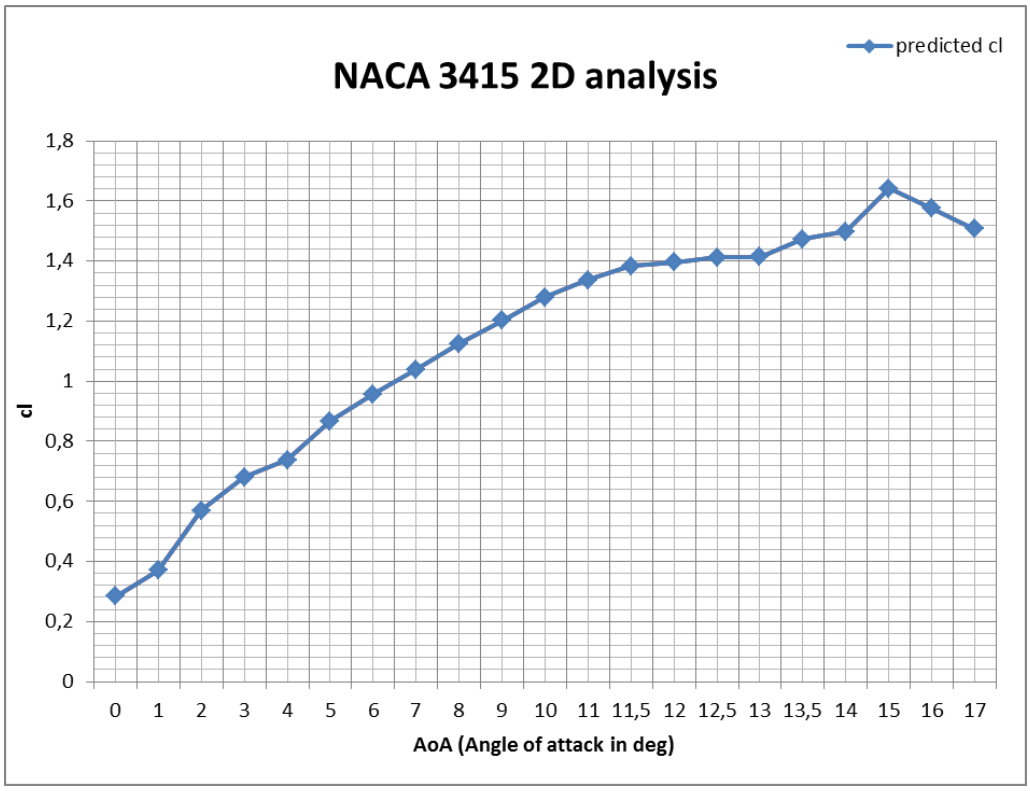

Figure 31: NACA 3415 2D analysis predicted lift coefficient

Figure 32 shows the predicted drag coefficient. Results also look very reasonable. Note how, like most drag curves, results are plotted until and AoA=13-14º only, as after those values drag coefficients begin to increase dramatically due to flow detachment and stall conditions and most results would lack accuracy. A rather exponential drag increase can be seen with the angle of attack increase.

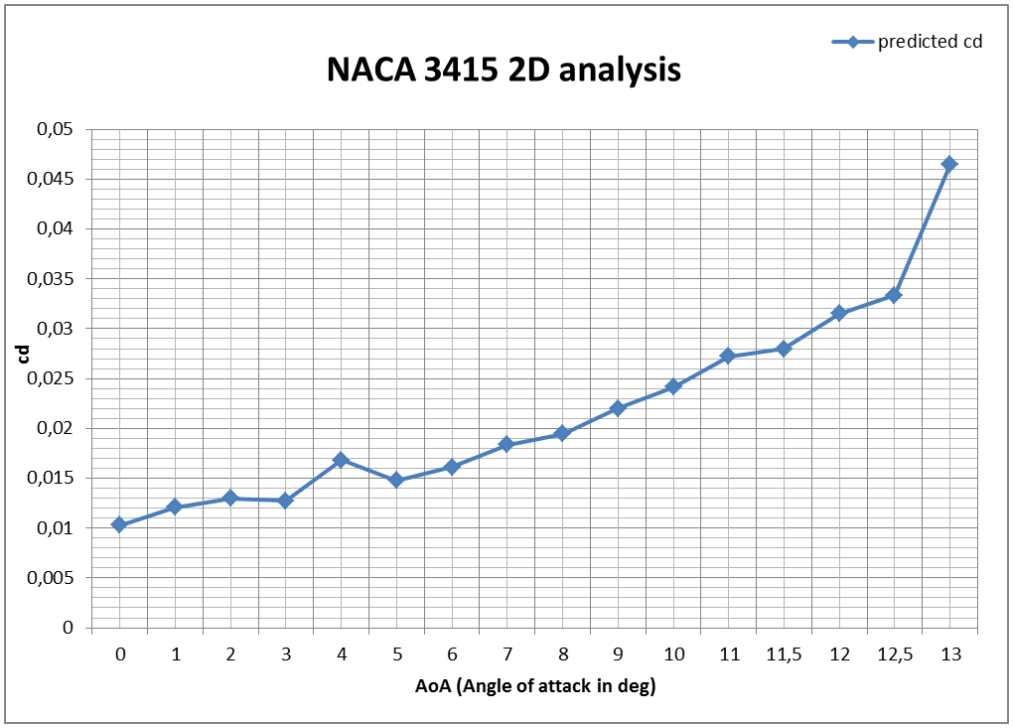

Figure 32: NACA 3415 drag coefficient 2D simulation results

As it has been explained in the time step discussion 3.2.3.5, this is an unsteady simulation, thus analyzing the lift coefficient's behavior over time does shed some light on the study. Below one can found the lift coefficient oscillation plots during stall progression.

Lift coefficient monitors show no cycling values for AoA =11º.

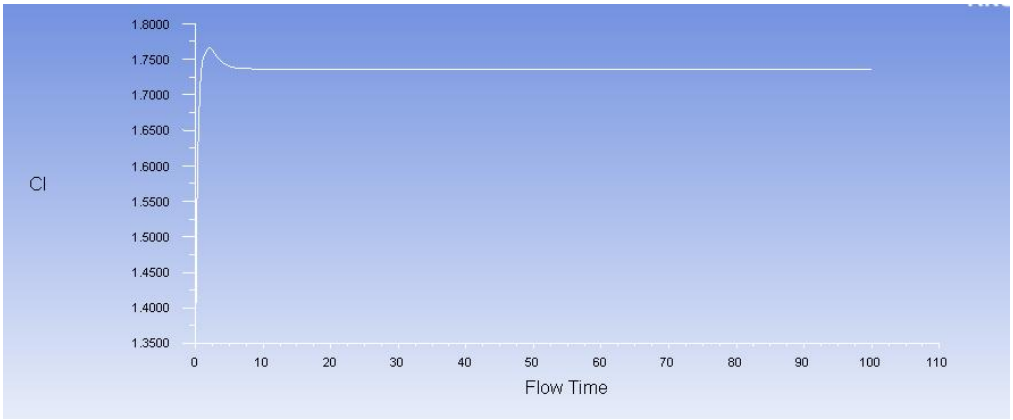

Figure 33: Lift coefficient performance during simulation flow time for AoA= 11º

For AoA=12º, the c_l begins to cycle but oscillation rapidly increases for AoA=12.5º, where the amplitude of the oscillations is 0.02. This means turbulence presence. Note that y-axis scales are different for every figure.

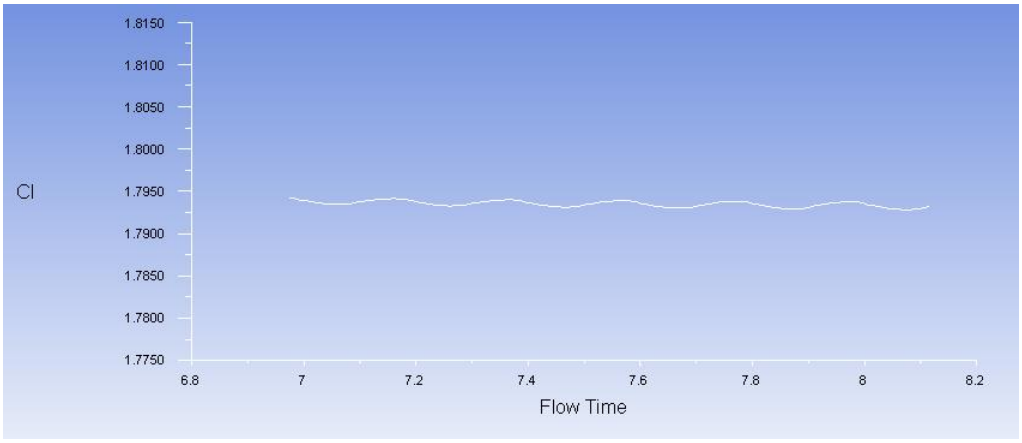

Figure 34: Lift coefficient performance during simulation flow time for AoA= 12º

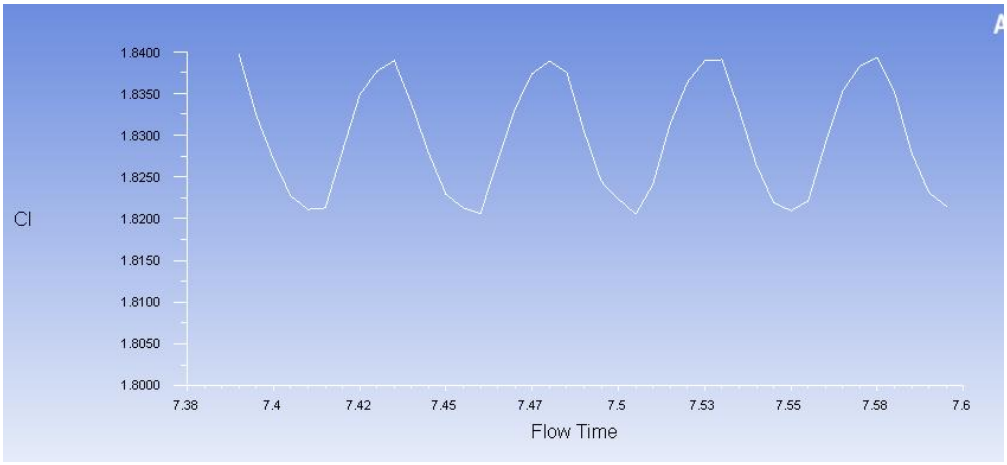

Figure 35: Lift coefficient performance during simulation flow time for AoA= 12.5º

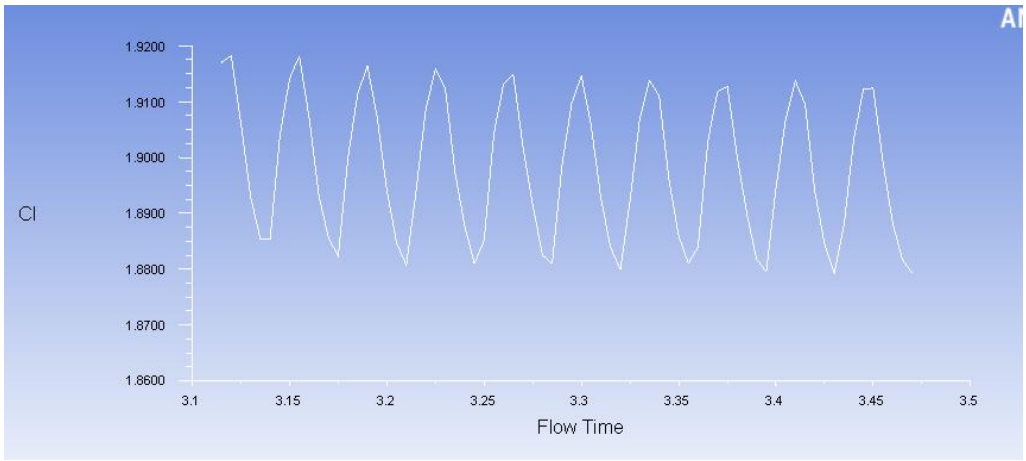

Figure 36: Lift coefficient performance during simulation flow time for AoA= 13.5º

For AoA=14º, amplitude of the oscillating lift coefficient is around 0.02 too. This means that the lift oscillation does not increase too much beyond this point, so that the transition into turbulent flow and boundary layer detachment occurs around 13º of angle of attack.

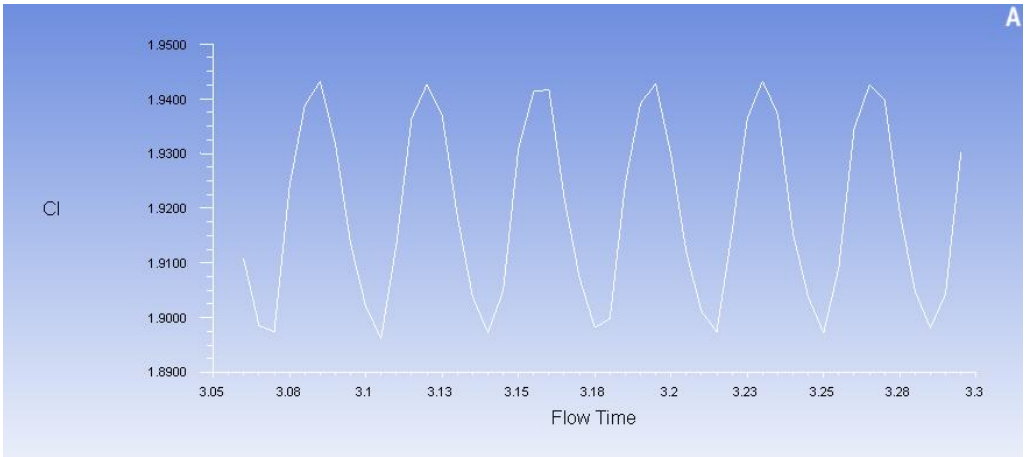

Figure 37: Lift coefficient performance during simulation flow time for AoA= 14º

Using the stall detection criterion exposed above, the detection of cycling values of lift and drag coefficients can be considered a symptom of the airfoil being in stall condition, thus the result of the 2D simulation is that the critical angle of attack of the airfoil is 13º.

3.2.5 Results verification

2D simulation results are verified with NACA 3415 experimental data found in reference [27]. The original lift coefficient against angle of attack chart can be found in the section 9 of the Annexes.

Figure 38 shows a very good correlation between simulation and experimental data in the linear range. However, the lift coefficient is overpredicted in the stall region, until it begins to decrease 2 degrees of angle of attack later than the experimental data. There are some studies that exclusively focus on CFD stall study, like reference [26].

Therefore, it can be said that the valid range of the simulations is until the critical angle of attack is reached. Around stall conditions, as it has been exposed, it is hard to predict the airfoil behavior thus gathered data has to be questioned.

As for the drag coefficient prediction (Figure 39), the shape of the curve corresponds very well with experimental data. The actual value of the drag coefficient is around a 10-25% higher in the simulation, but this proportion always stays the same and the increase of the drag is not erratic but it follows the same pattern as experimental data.

Considering that the **affordable** conditions of the simulation are pretty close to the **ideal**, it does make sense that results correlate well. The lift coefficient is overpredicted in the forces report, but having a look to the streamlines and especially studying coefficients oscillation in order to detect turbulence presence helps to determine the correct critical angle of attack. Causes of inaccuracies around stall conditions are attributable to bad turbulence modeling and this problem cannot be

solved from one day to another; it is actually one of the main focuses of attention of the CFD sector.

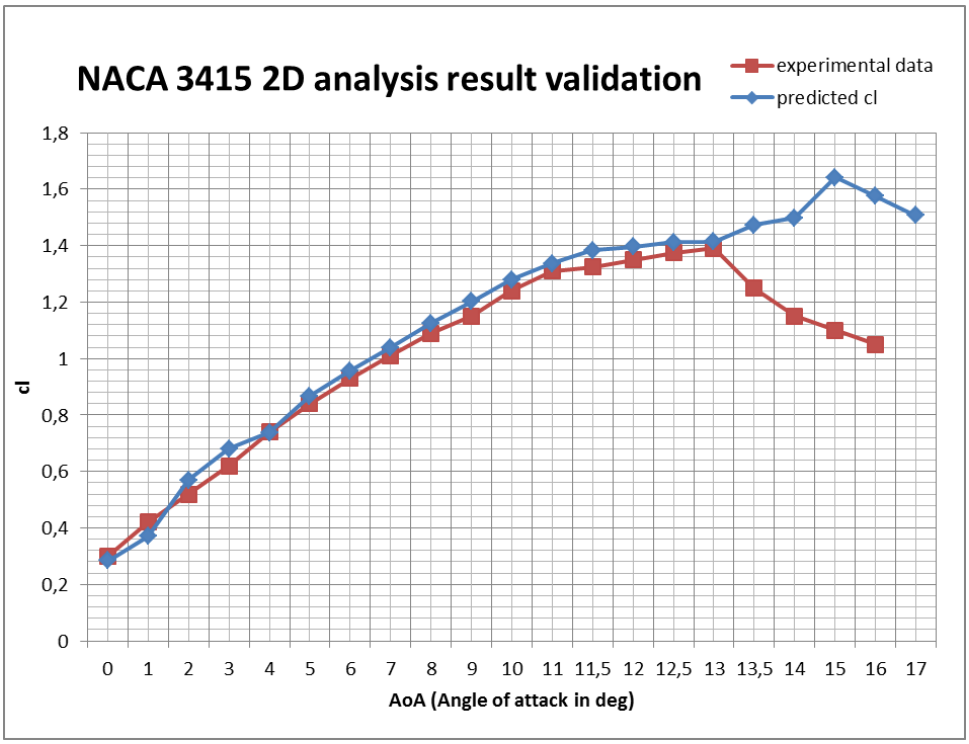

Figure 38: NACA 3415 2D simulation results comparison with experimental data.

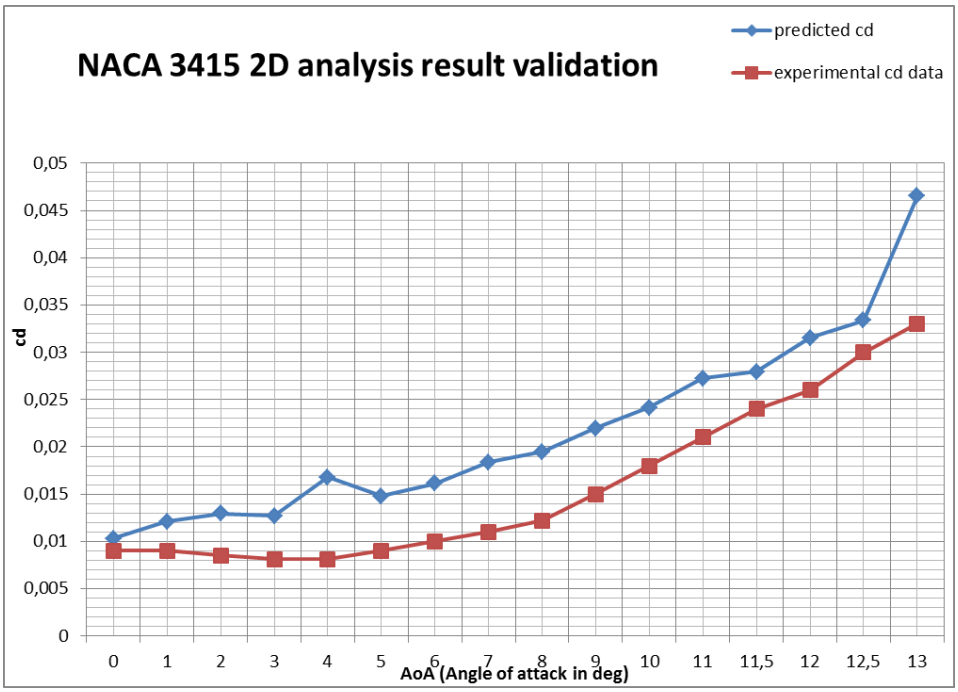

Figure 39: NACA 3415 drag coefficient 2D simulation results compared with experimental data

3.3 3D finite wing with VG preliminary simulation

3.3.1 Computer power limitations

A 16GB RAM machine and 3,1GHz i7 processor were used to carry out the simulations.

The computer was not able to create grids for more than $4 \cdot 10^6$ elements, and the solver just froze for solutions for meshes around that order of magnitude.

A $1 \cdot 10^6$ element was created and analyzed in transient conditions with a time step of 0.005 seconds. After 10 hours of simulation, only 2500 iterations were performed, which consisted in around 18 time steps and no significant data could be extracted, as it can be seen in Figure 40.

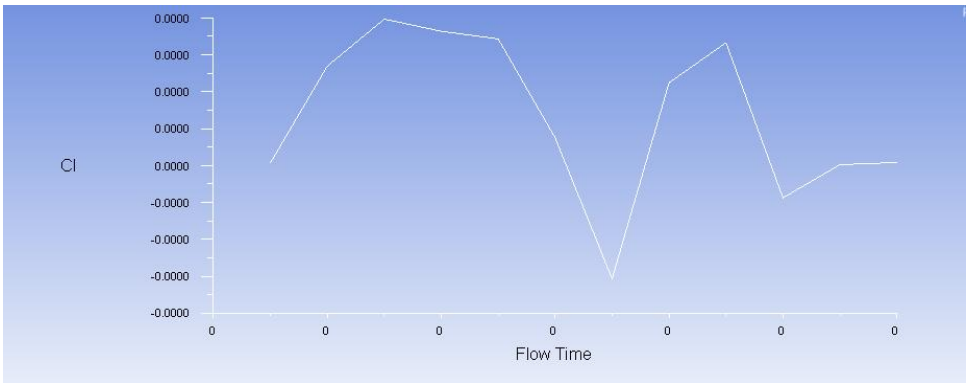

Figure 40: Lift coefficient monitor of a 3D transient analysis

Figure 41 clearly shows the convergence problems of the solution due to coarse, low quality mesh and turbulence model choice. It shows the process of convergence for 18 steps during 10 hours of simulation.

The fact that not even remotely close-to-ideal conditions will be achieved in the 3D simulations is evident. Computational power will be giving problems in every single step of the pre-process.

- Geometry volume control
- Mesh generation.
- No transient analysis available
- Solution slow convergence: a very coarse mesh with one million elements takes 10 hours to perform 18 time steps.

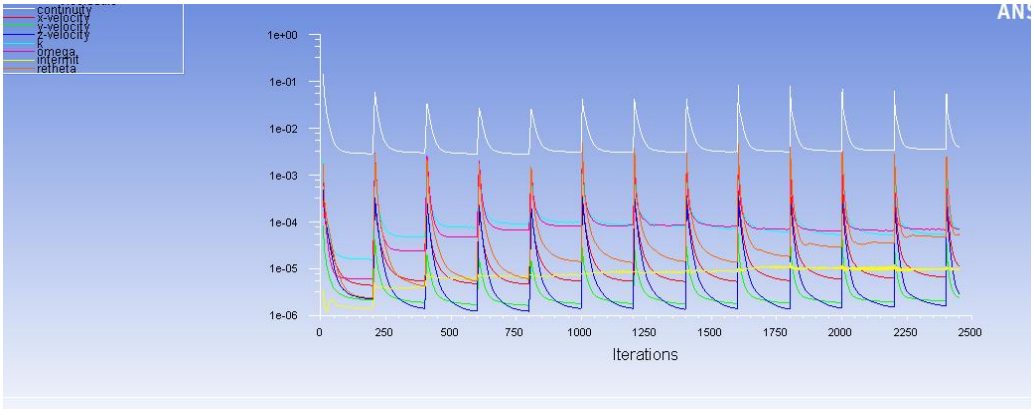

Figure 41: Slow and tedious convergence; scaled residuals of a 3D transient simulation

The preliminary study aim to perform 3D analysis had to be forgotten, but this section will still set the ideal criteria for the 3D analysis and it will show some wrong results to compare with experimental data.

Transient 3D analysis of the coarse mesh took about 3-4 hours to converge, which clearly shows the complexity of the simulations. If the coarse mesh took so much to converge, it is not even remotely possible to attempt a transient analysis with

3.3.2 Geometry modeling

3.3.2.1 Finite wing portion with VG

To begin dealing with only two VGs and study their effects and possibilities, and keeping in mind computational limitations, an approach with a portion of the wing is recommended, as trying to simulate the whole wing is a very bold choice.

Finite wing

Chosen configuration has been a 400mm wide finite wing containing 2 VGs separated by 100mm and located at 0.08 times the chord from the leading edge. The VGs have an angle of attack of 20º. This VG configuration has been chosen among some standard general aviation VG configurations. As computer power so far does not really allow to simulate these effects, any VG configuration is good to test the software.

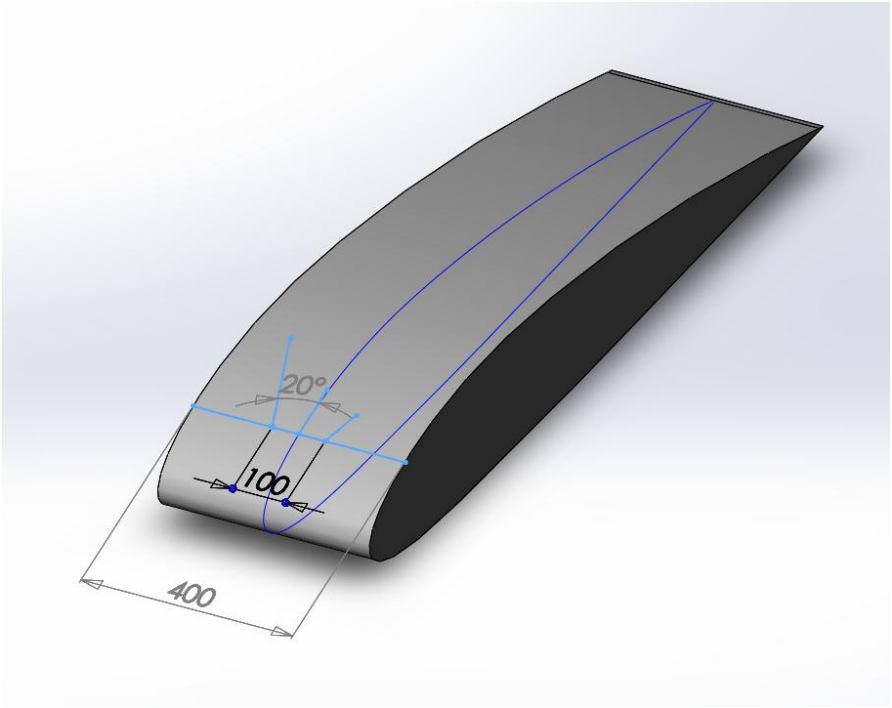

Figure 42: Portion of a finite wing with VGs used for the test 3D simulations

VGs

Rectangular, common state of the art vortex generators have been modeled to be attached to the wing portion. As this is a preliminary study, the shape and dimensions of the VGs are completely irrelevant, as long as they are fairly usual in ultralight aircraft.

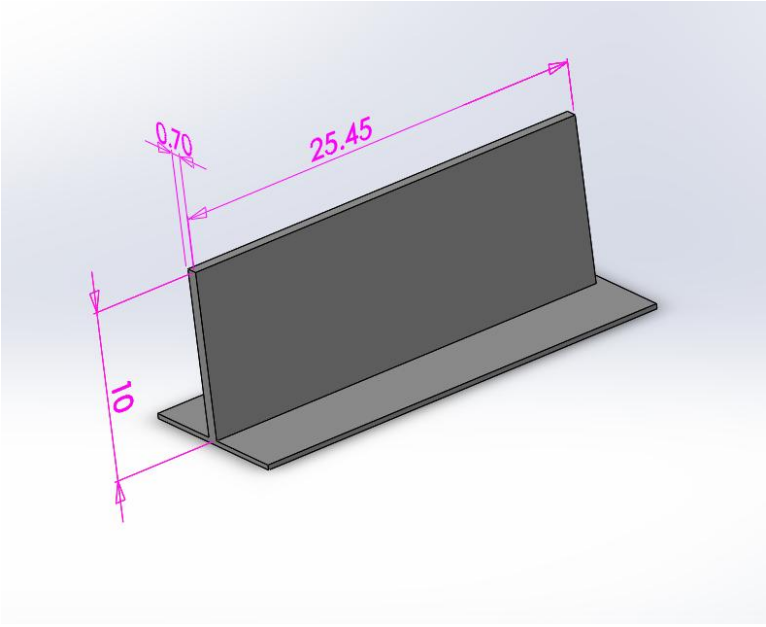

Figure 43: VG geometry modeled used for the test 3D analysis

Ideal volume of control

Following the 2D simulation results and bibliography, extruding the 2D mesh along the wingspan would have been a good solution. This ensures no interaction between walls of the volume of control and the wing itself. Figure 45 shows a good example of an ideal volume of control.

Affordable volume of control

As the ideal volume of control is unaffordable in terms of number of elements, it was narrowed to enclose the finite wing and most immediate surrounding flow. This entails some interaction between walls and wings, and it can not be measured. Inaccuracies in the results may occur but it is unknown if a volume of control too narrow does affect them, and up to what point. To mitigate this effect, boundary conditions in the walls are set to zero shear stress, instead of no slip conditions.

3.3.2.2 Whole wing analysis

As it will be clearly exposed later, geometry like Figure 44 is totally unaffordable as a decent mesh of the wing and its VGs would imply a massive number of cells – around the 10^7 order of magnitude.

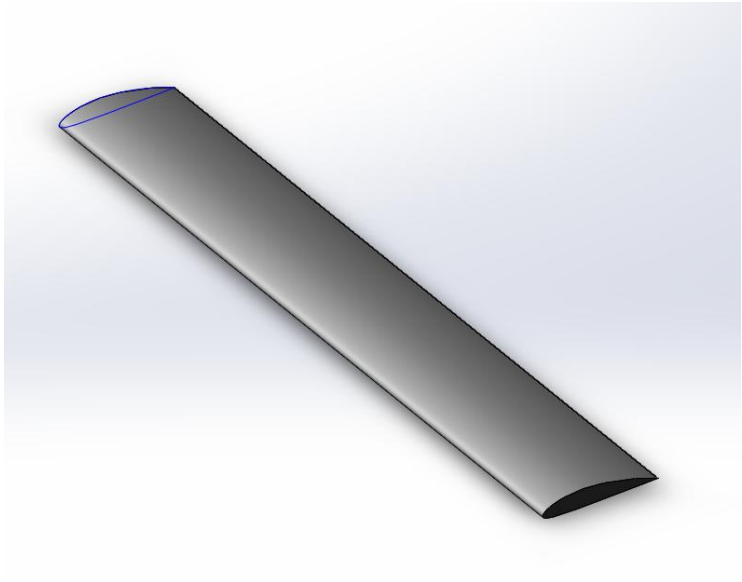

Figure 44: Full wing 3D geometry

3.3.3 Simulation criteria

3.3.3.1 Y+ calculation

For the 3D analysis, conditions regarding y+ are the same as the 2D analysis. It is a must that y+=1 for the simulations. The estimated wall distance for the first cell height is then calculated. Ideal conditions would be the ones found in Table 3, while affordable conditions for 3D simulations are the same as for 2D, corresponding to Table 5.

3.3.3.2 Model preference

Transitions SST (4 eq.) has been given reasonable results for the 2D analysis, and it's suitable for a 3D vortex generators analysis according to bibliography. Therefore, preliminary test 3D simulations will be carried out using this turbulence model.

3.3.3.3 Mesh

Ideal mesh

An ideal 3D mesh domain should be created following criteria exposed in [28]. An idea of the reference geometry and the domain size that should be used can be seen in Figure 45.

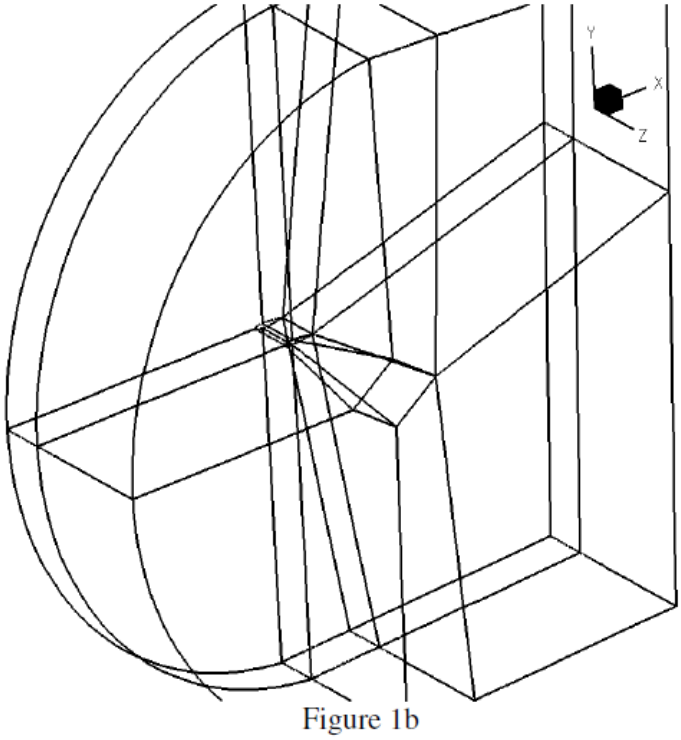

Figure 45: 3D finite wing reference geometry for CFD mesh

A proper vortex generator grid can be found in references [10] and [29]. This example found is using a 18 million cell grid; something which is not in the range of this academic study.

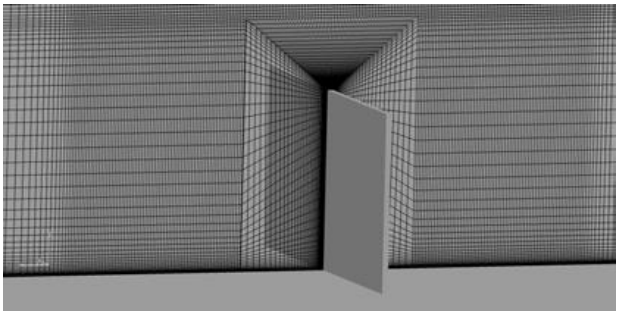

Figure 46: Cross section image of a 18 million element grid for a single VG

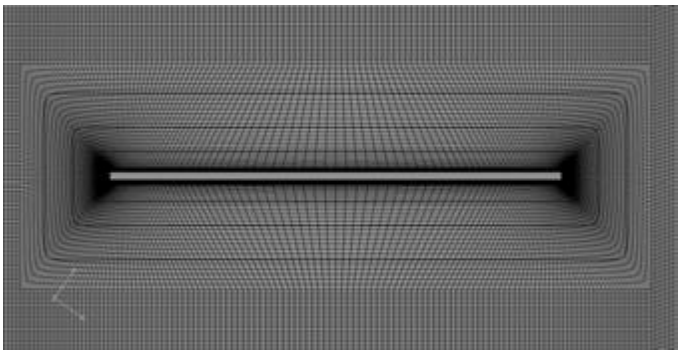

Figure 47: Horizontal section of a 18 million cell grid for a single VG

Affordable coarse mesh

A one-million-element low-quality mesh was generated to at least obtain some results. It is shown in Figure 48. Note that walls were set to null specific shear stress in order to not alterate the velocity countour.

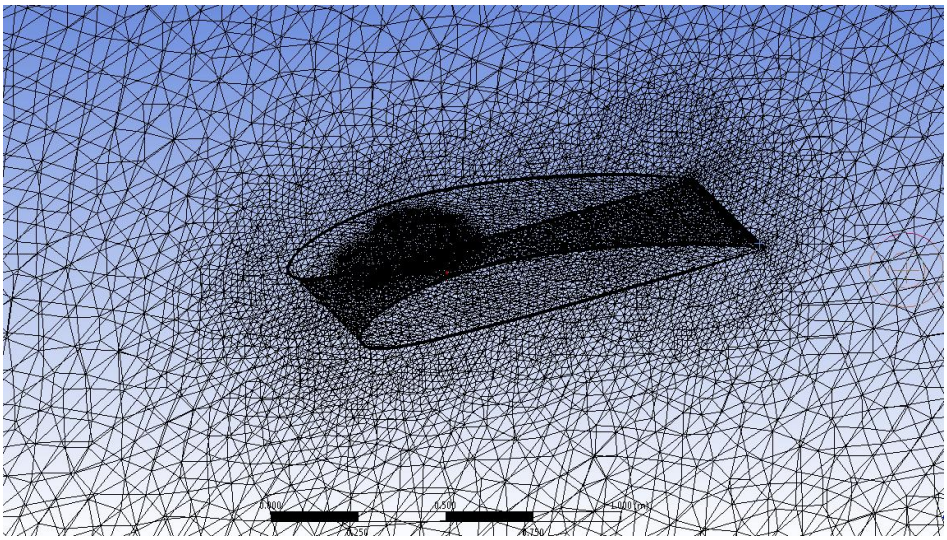

Figure 48: Coarse geometry mesh used for a preliminary 3D CFD simulation

Some refinement was tried to be applied around the VG geometry and along the downstream flow (Figure 49), but still this refined section is way too coarse in comparison with the needed refinement shown in Figure 46.

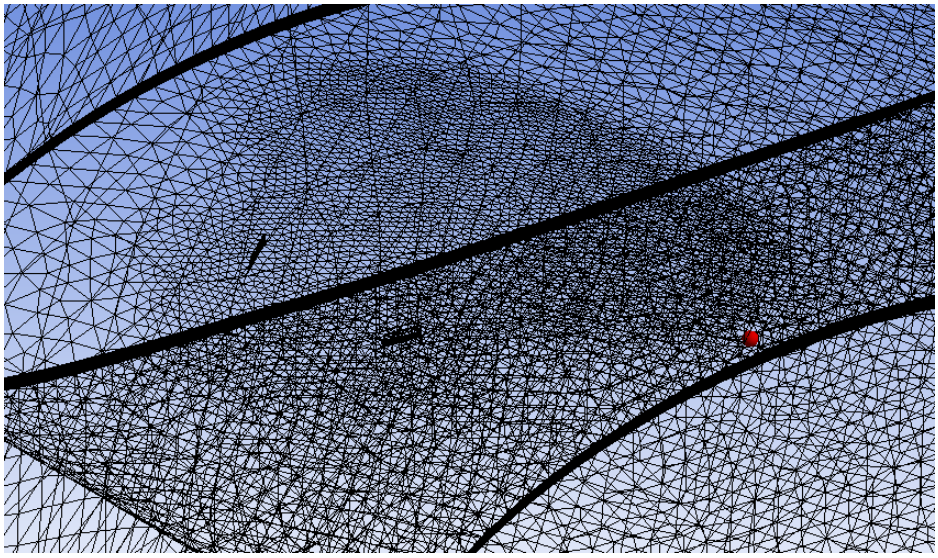

Figure 49: Coarse mesh refinement around VGs used for preliminary CFD simulations

3.3.3.4 Grid dependence

Results were clearly grid dependent, as a tiny change in the grid parameters can radically change the simulation results. Results were not corresponding with experimental data using a coarse mesh, but using a very coarse mesh they were even worse. This evidences a lack of computer resources to perform this kind of analyses.

3.3.3.5 Time step

The same criterion is applied as the 2D simulations. Time step should be computed as:

$$\Delta t \geq \frac{u}{\Delta x} \geq 1.456 \cdot 10^{-5} s$$

However, computational power limitations do not allow performing transient analysis.

3.3.3.6 Stall prediction

Stall in 3D will be predicted following the same criteria as 2D. However, 3D vortex generated in the wing tips might create turbulence and cycling lift and drag coefficient values from the very start, thus assuming that the presence of turbulence entails stall would lead to wrong results. Hence, stall has to be predicted only through lift coefficient decreasing with AoA increase and streamlines / velocity contours observation.

3.3.4 Preliminary simulation results and verification

Analyses were carried out for a 40cm finite wing in clean configuration. Table 8 shows the results obtained for various angles of attack and a contrast with experimental data. Even that the simulations were carried with VGs, results are contrasted with non-VG wing experimental data, as no other information was found. Wing experimental data is found in section 10 of the Annex.

Angle of attack	Cl Experimental data	Cl 3D simulation
0º	0,25	0,37
13º	1,1	0,65
15º	1,21	0,73
20º	1,2	0,86
25º	1,05	0,90

Table 8: 3D preliminary simulations result contrast with experimental data

As it can be seen, the correlation between experimental and simulation data does not exit. The reason for the lack of correlation is not that experimental data has no VG, and the simulation does have it. Other simulations were carried out without VGs and results also differed. Moreover, VGs do not affect the global lift coefficient as much as a 40% of the total value.

Simulated lift coefficient begins higher than experimental but it increases way slower along with angle of attack. Moreover, simulations does not detect the wing stall point at AoA= 17º and lift just keeps growing. Even at AoA=25º, the CFD analysis states that the flow is attached to the wing and still generating lift. A streamline plot of the velocity (at AoA=25º) around the wing has been generated to confirm how far those results are from reality. Not finding detached flow in a wing at an angle of attack of 25º in Figure 50 is a clear symptom that the pre-processing of the analysis has not been done correctly. For such values of angles of attack, flow should be detached and a wing should not be producing lift.

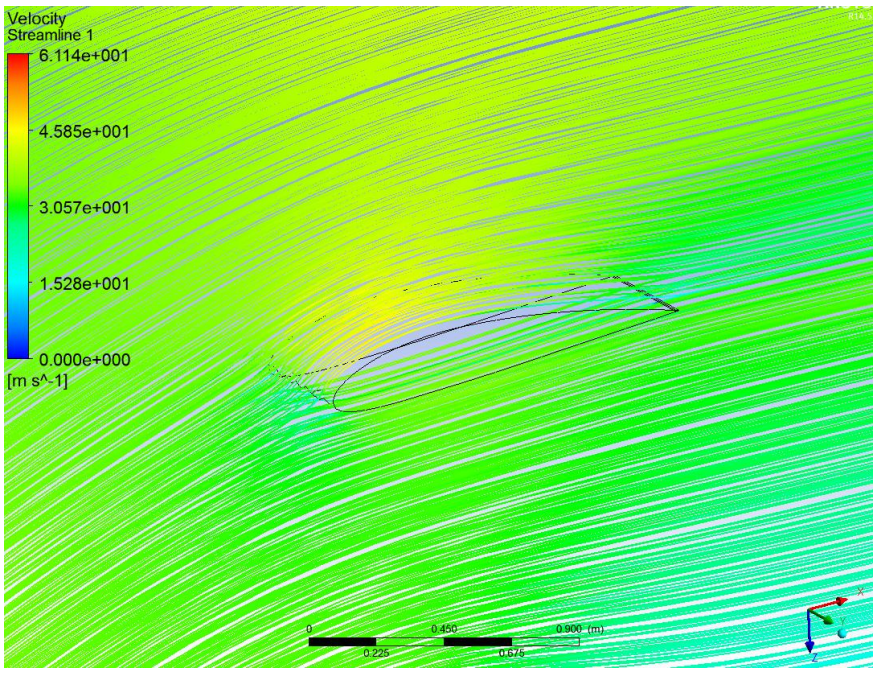

Figure 50: CFD analysis; 3D flow accross a wing for an AoA=25º - wrong results!

3D results need a deep review as they don't make any sense when performed far from ideal conditions. A more powerful computer along with more software knowledge is needed to pull out decent results from such complex simulations.

PART IV: EXPERIMENTAL TESTS

4.1 Experimental tests introduction

Preliminary flight tests have been carried out with the Alto TG912 ULS aircraft.

Flight tests with and vortex generators can focus in a lot of parameters and variables, but due to the project's limitations, only one VG configuration will be analyzed and the three aspects where the tests will focus will be:

- Stall speed
- Stall behavior
    - maneuverability of the aircraft during stall progression
    - part of the wing that begins to stall
    - flow detachment observation during stall
- Overall aerodynamic behavior

This is a qualitative approach and its results have to be taken cautiously, while understanding that some uncontrollable factors may have affected the outcome of the tests. Those factors could include:

- Anemometer lack of precision or delay
- Variable air characteristics between tests
- Change in winds, gusts, and turbulence between tests
- Minimal aircraft weight changes between tests

All flight tests were recorded on video.

4.2 Experimental tests results justification

The actual aim of the flight tests is gathering real data to contrast future 3D simulations. Implementing VGs in an ultralight wing is expected to cause different behavior on the aerodynamics, different stall conditions, and lower stall speeds. All the data regarding the three aspects mentioned in the above section is intended to be used to compare and verify 3D wing simulations. Flight test's aim is not to implement a large amount of VGs configurations, but to give support to the simulation stage and take the final decision regarding the optimal VG configuration for the given ultralight model.

4.3 VG choice and construction

Usually VGs are installed in couples, as the 3D simulation geometry shows or Figure 13 illustrates. However, VGs used for experimental tests consisted in a single piece made of aluminum that could already be used as two VGs looking at each other, consisting in two sharp fins forming an α wing with the freestream flow direction. This was done because, as it has been seen, VG kits are rather expensive and the author decided to build his own VG devices using an aluminum flat plate and proper tools. Pictures illustrating the process followed by the author to construct and mount the devices into the aircraft wing can be seen in the section 12 of the Annexes.

Figure 51: Picture of the VGs used for experimental tests

Current state of the art parameters and dimensions have been used to design the vortex generators. Data to copy the design of VGs was obtained visually from other aircraft in the hangar.

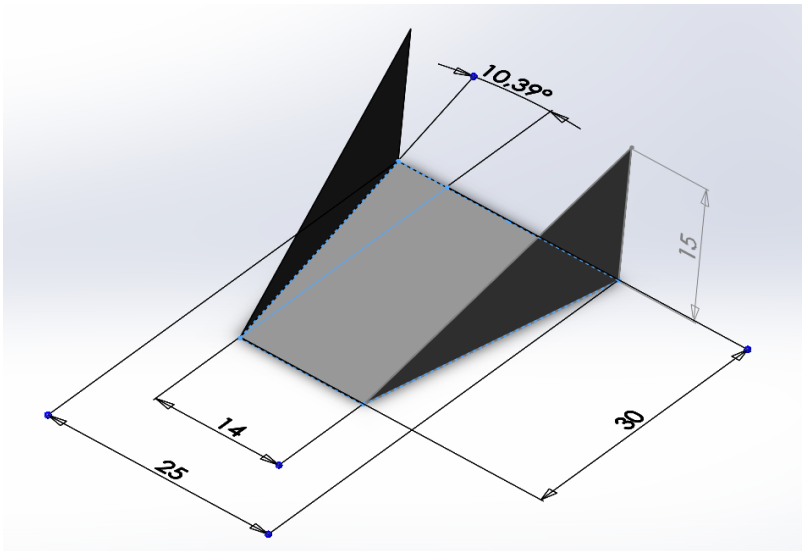

Figure 52: 3D VG model used for experimental tests

4.4 Experiment setup

4.4.1 Casette tapes setup

To see the air conditions all over the wing, the whole right wing was covered by glued cassette tapes. Four rows of ~12cm cassette tapes were stick along the wing, causing no effect to the wing aerodynamics but always pointing to the local wind direction.

Interpreting the cassette tapes movement is not complex.

- Tapes straightly pointing backwards – in the same direction of the free-stream velocity – denote laminar flow.
- Tapes beginning to vibrate and oscillate are a consequence of the presence of turbulent flow around them.
- Tapes pointing against flow velocity or randomly moving without having a steady position mean detached flow in the zone where they are placed.

4.4.2 VGs setup

To fully appreciate the different behavior of a wing with and without VGs, a row of 19 VGs were mounted from the wing tip to two meters from the wing tip. A wing region of around 1.5m between the cabin and the first VG was left so the behavior of the stall progression without VGs could be appreciated at the same time, thus recognizing different flow characteristics with a quick glance would be possible.

VGs were placed every 10cm, and they were situated at 0.08 times the chord length from the leading edge. VGs had to be mounted in both wings, as causing intentional stalls with an asymmetric wing configuration could lead to dangerous spins.

Figure 53 clearly shows the configuration of the wing when VGs and tapes were installed.

Figure 53: Wing setup of the ultralight used for flight tests

4.5 Flight tests without VG

Before installing the VGs, a first test was performed to observe airplane's clean configuration stall characteristics. Noticeable changes regarding stall speed, stall behavior and general aerodynamic behavior were reported.

4.5.1 Stall speed

Flight manual provided by the manufacturer ensured a stall speed of 75 km/h, but after ten dynamic and static intended stalls, the mean velocity at which the aircraft began to stall was 78 km/h. Stall is considered to happen when the airplane vibrates, no longer feels maneuverable, has to be pitched down to gain speed and when around 30% of the tapes are disordered.

4.5.2 Stall behavior

If the nose of the airplane was held during stall, the vibration persisted and the nose of the airplane fell down. The airplane then behaved like a wounded bird until some speed was gained. The nose drop without VGs was rather sudden and violent, and ailerons had a very little efficiency, as flow was detached in the wings.

Figure 54, Figure 55 and Figure 56 clearly show the flow transition during stall progression. Flow detachment is clearly reported to start in the middle part of the wing (see last row of tapes in the middle part of the wing Figure 55), and as stall progresses (Figure 56) flow detachment advances to the second and third row of tapes and expands to the root of the wing. Stall also hits half of the section in the aileron, but the flow around the wingtip remains attached – which is actually a good

wing design as the airplane has at least a little of aileron control during stall. The flow remains attached in the wingtip zone probably thanks to the torsion of the outer part of the wing and the vortex generated by the wingtip itself. The flow in the VG zone remained attached at any angles of attack and conditions.

Figure 54: Experimental tests without VG: low speed flying

Figure 55: Experimental tests without VG: stall progression

Figure 56: Experimental tests without VG: fully stalled wing

4.6 Flight tests with VG

4.6.1 Stall speed

Stall speed was noticeably reduced with the implementation of VGs: 70 km/h. The aircraft could handle the 75-80km/h velocity region with plenty of operative control surfaces and maneuverability, something that for a clean configuration previously was an almost-stall situation hence the noticeable stall speed reduction was about 5-7 km/h.

4.6.2 Stall behavior

Stall behavior was clearly gentler than without VGs. As half of the wing's flow remained attached, it was harder to make the airplane fully stall, as VGs helped the ultralight feel comfortable in the low speed regime. A lot more effort had to be put into pitching the nose up to stall the airplane, and still the airplane did not drop the nose like the previous test.

Another important factor is the stall progression. With VGs, flow detachment clearly began in the root of the wing. Then it progressed through the wing until the middle part of the wing, where VGs were installed. Then, whatever the pilot could do was not enough to see detached flow behind the VGs. By checking Figure 59 – the moment when the stall was stronger- it can be seen that the flow is detached in a 60% of the wing root (it even hits the first row of tapes) but it still remains attached 2m from the wingtip.

Comparison between Figure 56 and Figure 59 is the strongest and most graphical proof of the vortex generators effects in the ultralight.

Figure 57: Experimental tests with VG: low speed flying

Figure 58: Experimental tests with VG: stall progression

Figure 59: Experimental tests with VG: fully stalled wing

4.6.3 Overall behavior

The ultralight itself felt a lot more maneuverable. It was capable of handling lower speeds a lot better and aileron control was fine during stalls, low speed flying, take-off and landing.

The lift-off occurred earlier than expected as the wing was capable of generating lift at an earlier velocity than expected.

The final approach was carried out like usually, setting full flap at 200ft AGL, with a theoretical approach speed of 100 km/h. With VGs, the airplane wanted to go a little slower and was capable to perform the approach at 90-95km/h with no loss in aileron control. The airplane touched the ground at an abnormal speed of 80 km/h instead of 90-95 km/h because during the flare it was hard to put the ultralight down as it just kept flying over the runway due to VGs high-lift effects and ground effect. These reductions in the landing speed entailed a considerable reduction in the landing distance, as breaks were applied and the aircraft was able to come to a stop earlier than usual.

No cruise velocity difference was spotted as a consequence of the additional drag that VGs should be creating. This verification was done by setting the engine power to 5000rpm and the variometer to 0 ft/min for VG and non-VG configurations. The indicated speed set by the anemometer was roughly the same for both cases.

PART V: CONCLUSIONS

5.1 Conclusions

5.1.1 Previous study and pre-processing simulations

The aim of the study was to set the criteria and procedures needed to properly study vortex generator's behavior and performance for a given ultralight aircraft model.

The previous study carried out by this paper concludes that the study of flow transition and stall conditions is very complex and has to take into account a lot of variables. The main reason is that one of the largest and most popular fluid mechanic problems quickly arises: turbulence modeling.

As this previous study is a mere previous step towards accurate CFD simulations and / or experimental tests, there are several parameters that have been labeled as critical in the progression of a study involving 3D sub-boundary layer effects.

- Reynolds number

When the Reynolds number varies, everything in the fluid changes. Studies, airfoil and wing data, plots, certain equations are only valid for a certain range of Reynolds numbers. Special attention has to be paid to this non-dimensional number.

- Y plus parameter

In CFD simulations, the study of the y plus parameter along with the turbulence modeling requirements is a must to predict the boundary layer behavior. The importance of the wall treatment in airfoil and wing analysis has become evident.

- Courant number

In transient simulations, the courant number criterion is very important to estimate the time step that has to be used and detect all the phenomena that is going on – specially in turbulent conditions. To capture cycling values of coefficients it is crucial to use correct time step setups.

Moreover, when it comes to the simulation pre-processing, the 2D analysis clearly shows that when input conditions are close to the ideal situation, simulation results tend to get closer to experimental data. On the other hand, as the 3D analysis shows, when computational power limits the input conditions such as mesh number of cells, results quickly move away from the real solution.

Therefore, as a conclusion, special emphasis has to be put in the pre-processing of the simulations, especially regarding:

- Mesh

A well-refined and optimal grid ensures that the turbulence model predicts correctly and it surely helps equation convergence, reducing simulation time and improving result's accuracy.

Around 10^5 elements would be needed to obtain reasonable results in a 2D simulation, whereas around 10^7 elements would be needed to accurately predict vortex generators physical effects in a 3D simulation. Boundary layer inflation refinement is needed, as well as a geometry wide enough as not to influence the results.

- Turbulence model

The optimal turbulence model to simulate the problem posed by this paper is the Transition SST (4 equation) model. The k-ω SST 2 equation model is also very suitable and has a faster convergence. The difference between those two is the two extra equations added to the Transition SST model, which should presumably add accuracy to the model.

5.1.2 Simulation results

According to verifications of the section 3.2.5, 2D simulation results match very well experimental data because simulation conditions (y+, mesh number of elements, mesh quality, transient analysis) are close to the ideal simulation conditions. The fact that lift is over predicted after the critical angle of attack is reached remains unclear, but it is a very common problem among CFD airfoil simulation.

As it has been seen in 3.3.4, the fact that 3D analyses do not return reasonable data was easily predictable. The analysis were carried in steady conditions due to computational limitations, while stall and post-stall conditions have to be run in transient analysis to evaluate the flow transition and stall progression over time, so steady simulations results are only a little reasonable for low angles of attack, where the flow is laminar. Moreover, the mesh was not fine enough as to capture such tiny vortex effects even if the turbulence model was good.

3D simulations, if wanted to be performed properly, take a lot of computer power and should always be avoided in everyday computers, as results will take up a lot of time to come and might not be even close to real solution. Higher computational power is definitely needed in order to simulate vortex generators effects.

5.1.3 Flight tests results

Flight tests with vortex generators successfully showed the advantages of this device. A 5-7 km/h reduction in the stall speed was detected and better stall progression was spotted in terms of aileron maneuverability. This can be translated into shorter take off runs and landing distances, which are both crucial factors in

general aviation. Vortex also caused a more gentle stall and general aerodynamic behavior which confirmed the better overall ultralight performance predicted by the consulted sources.

Stall with VGs was beginning in the root of the wing and flow remained attached in the VGs region for any angle of attack. This gives crucial information regarding the real flow behavior during stall conditions. The video recording material pointing towards the wing with tapes and the anemometer can be very useful for future studies and experimental data verifying. The qualitative approach of the experimental tests gave a rough idea of the real life effects of the devices, which can be used to contrast 3D simulations in the future.

5.2 Recommendations

To who is interested in carrying out a study involving vortex generators, the author of this paper strongly recommends:

- To deeply study turbulence modeling bibliography regarding transitional flows and boundary layer simulations, as there is a lot of information available, as well as CFD forums with expert users that provide nice knowledge.
- To consult bibliography related to vortex generators configuration studies, as there is a lot of studies (done with CFD and / or experimentally) done since this technology or concept was invented – more than 50 years ago.
- To pay special attention to the parameters mentioned in the conclusions in order to have a reliable simulation or experimental tests setup. If the previous steps are done incorrectly and a criterion is wrong, further studies will not return accurate data.
- To follow the given guidelines regarding simulations pre-processing to avoid the "garbage in, garbage out" phenomena. Working on refining the conditions of the simulation is primordial to obtain accurate results.
- Use the software ICEM CFD to create the geometry and the grid as it is more efficient than Ansys mesh tool.

Regarding flight tests, it is recommended to perform more flight tests to analyze the additional drag creation and the stall progression. Different types of VGs should be used and they should be placed in different positions to deeply study the pros and the cons of each configuration, and contrast the results with simulations. Experimental tests (they can also be carried out in a wind tunnel) and simulations have to focus on the same aspects in order to get stronger evidence of the effects or notice the lack of correlation between CFD and real life.

5.3 Study continuation: future tasks

Assuming that enough computational power can be found to carry out the 3D required simulations, the preliminary study performed in this paper would lead to a complete study of vortex generators effects and concluding a reasonable VG configuration for the given ultralight model for its optimal performance.

5.3.1 Task identification

Tasks that are left to complete a deep study regarding vortex generators effects in ultralight aircraft are exposed below.

#	Tasks	Weeks	Precedent
1	High power computer solution implementation	2	-
2	High quality mesh controls research	1	-
3	3D Simulation pre-processing	4	2
4	Iterative simulation (first stage)	6	3
5	Result post-processing (first stage)	1	4
6	Iterative simulation (second stage)	6	5
7	Result post-processing (second stage)	1	6
8	Experimental flight tests	4	7
9	Result analysis and general post-processing	2	7, 8

Table 9: Future tasks to be carried out, weeks of duration and precedent task

The iterative simulation task refers to the iterative process of creating a geometry, mesh and solution conditions, resolving the system, post-processing the result and repeating the task depending on the previous results obtained.

Note that two simulation stages have been considered, but more simulation stages may be needed in case that problems arise or inconclusive results are obtained.

5.3.2 Gantt

Considering two simulation stages, the complete study could be done and reasonable conclusions could be drawn in about 26 weeks (half a year).

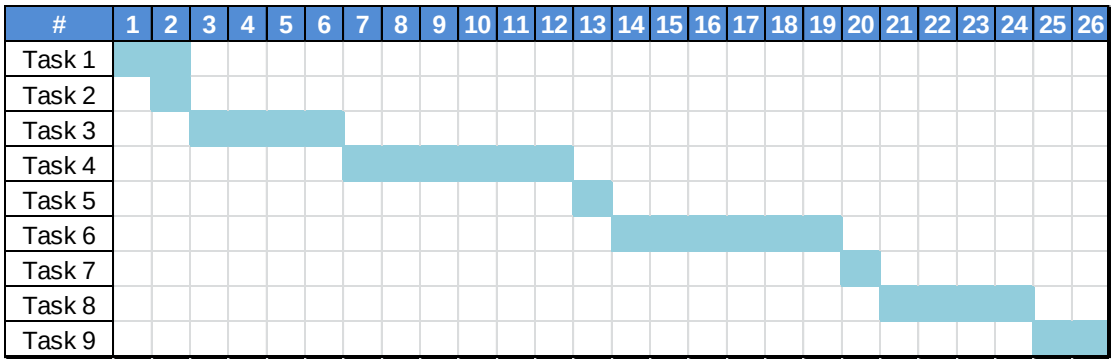

Figure 60: Gantt diagram of the future tasks to be completed

5.4 Economic and environmental implications

5.4.1 Budget

The most important expense of the project would be purchasing a Mini-cluster high value performance computer to carry out the simulations. This would have a cost of **32.000 EUR** [30]**.** There would be an option to rent a high performance computer with the same aim, or look for universities or research teams interested on running the simulation.

The cost of the experimental tests is computed at an average rent rate of 150 EUR per hour of flight. VG kits to be mounted in the aircraft could be either manufactured (like this preliminary study) or bought online – where they cost around 200 EUR per kit.

In document 3 Budget, the rest of economic requirements to perform the full study are exposed.

5.4.2 Environmental impact aspects

Although it has not been detected during experimental flights, VGs implementation in ultralight aircraft are reported to increase drag during cruise [16]. Cruise speeds are sometimes decreased by 1-3 km/h, which means a relative 0.5% change. If the ultralight pilot wanted to cruise at the same speed as the clean configuration, an increase of 2-3% in the fuel consumption could occur, along with the inherent increase in emissions. Note that no reports concerning this topic have been found, whereas estimating the real environmental impact of adding VGs to an ultralight aircraft can be really tedious and is influenced by many other factors. However, it can be concluded that VGs do not have a positive impact in the environment; they rather have a slightly negative or null one. Active vane vortex generators, where the devices are active only during approach and take-off and are hidden during cruise, could be a good solution to tackle this problem.

The author also wants to point out the fact that 3D modeling and CFD simulating is more energetically efficient than building prototypes and testing them in the wind tunnel or flight tests. Generally speaking, simulations usually contribute to avoid unnecessary experimental tests. The amount of electricity that a computer consumes (even if it is a high performance one) generates fewer emissions than an ultralight engine during flight tests and a wind machine engine during tests in a wind tunnel. CFD simulations are a more efficient and agile way to work on aircraft devices optimization. Moreover, more parameters can be controlled during computer simulations than in experimental tests, where a lot of non-ideal factors play a role too.

6. REFERENCES

[1] H. ABBOTT, A. VON DOENHOFF "Theory of wings Including a Summary of Airfoil Data." Dover Publications, 1959.

[2] V. TVEITERÅS, "Numerical Study of the Interaction of Flow over Two Airfoils in Relative Motion", 2011.

[3] S. B. POPE, "Turbulent Flows". UK: Cambridge University Press, 2000.

[4] AEROSPACE AND OCEAN ENGINEERING, "Airfoil and Wing Properties"

[5] "Wing Design Parameters." [Online]. Available: http://adg.stanford.edu/aa241/wingdesign/wingparams.html. [Accessed: 27-May-2015].

[6] "Factors that Lower or Raise the Stall Speed of Aircraft." [Online]. Available: http://www.experimentalaircraft.info/flight-planning/aircraft-stall-speed-1.php. [Accessed: 27-May-2015].

[7] D. C. WILCOX, "Turbulence modeling for CFD", 3rd ed.

[8] "CFD Online - Y-Plus Wall Distance Estimation." [Online]. Available: http://www.cfd-online.com/Tools/yplus.php. [Accessed: 25-May-2015].

[9] ANSYS INC, "Theory Guide" 2010.

[10] U. FERN, "Fluid Dynamic Characterization of Vortex Generators and Two-dimensional Turbulent Wakes" October, 2013.

[11] D. E. STEIN, "Vortex Generators" pp. 1–5

[12] "Wind turbine blades with vortex generators" 29-Mar-2011.

[13] F. VON STILLFRIED, "Computational fluid-dynamics investigations of vortex generators for flow-separation control". Doctoral Thesis.

[14] O. LOGDBERG, "Vortex generators and turbulent boundary layer separation control". October, 2006.

[15] AVWEB, "Vortex Generators: 50 Years of Performance Benefits." [Online]. Available: http://www.avweb.com/news/features/Vortex-Generators-50-Years-of-Performance-Benefits-221566-1.html. [Accessed: 25-May-2015].

[16] M. BUSCH, "Vortex Generators: Band-Aids or Magic? - AVweb Features Article." [Online]. Available: http://www.avweb.com/news/reviews/182564-1.html. [Accessed: 26-May-2015].

[17] "Efficiency: Stuck on vortex generators - AOPA." [Online]. Available: http://www.aopa.org/News-and-Video/All-News/2013/January/1/Efficiency-Stuck-on-vortex-generators. [Accessed: 26-May-2015].

[18] "Installation of Vortex Generators." [Online]. Available: http://www.vortex-generators.com/installation-of-vortex-generators.html. [Accessed: 26-May-2015].

[19] DIRECT FLY, "Flight manual Alto TG912"

[20] DIRECT FLY, "Alto 912 TG Ultralight Specifications." [Online]. Available: http://www.directfly.cz/index.php?option=com_content&view=category&layout=blog&id=34&Itemid=62&lang=en. [Accessed: 25-May-2015].

[21] CORNELL UNIVERSITY, "Fluent - Flow over an Airfoil." [Online]. Available: https://confluence.cornell.edu/display/SIMULATION/FLUENT+-+Flow+over+an+Airfoil-+Problem+Specification.

[22] A. BAKKER, "Lecture 7 - Meshing" Presentation, no. 2002, pp. 1–35, 2006.

[23] B. FELLMAN, "3 Meshing Strategy," pp. 38–59.

[24] P. CHOUGULE and s. R. K. NIELSEN, "Simulation of flow over double-element airfoil and wind tunnel test for use in vertical axis wind turbine," J. Phys. Conf. Ser., vol. 524, p. 012009, 2014.

[25] W. SKRZYPIŃSKI, M. GAUNAA, N. SØRENSEN, F. ZAHLE, "Modelling of unsteady airfoil aerodynamics for the prediction of blade standstill vibrations," 2012.

[26] J. PETRILLI, R. PAUL, A. GOPALARATHNAM, N. FRINK, "A CFD Database for Airfoils and Wings at Post-Stall Angles of Attack," AIAA Pap., no. 919, 2013.

[27] A. P. BROEREN, M. B. BRAGG, "Effect of Airfoil Geometry on Performance with Simulated Intercycle Ice Accretions," J. Aircr., vol. 42, no. 1, pp. 121–130, 2005.

[28] A. SPENTZOS, G. BARAKOS, K. BADCOCK, B. RICHARDS, P. WERNERT, S. SCHRECK, M. RAFFEL, "CFD Investigation of 2D and 3D Dynamic Stall" AHS 4th Decenn. Spec. Conf. Aeromechanics, 2004.

[29] U. FERNÁNDEZ-GÁMIZ, G. ZAMORANO, AND E. ZULUETA, "Computational study of the vortex path variation with the VG height".

[30] ANSYS INC., "High Value Performance Computers for Simulation"